Establishing a human *in vitro* model of T cell exhaustion

Sterre van Wierst

MSc Cancer, Stem Cells & Developmental Biology

Student ID - 6142389

Under supervision of Dr. Yvonne Vercoulen – Utrecht University

And the daily supervision of Stephanie van Dam, MD MSc

Examiners: Dr. Yvonne Vercoulen – Utrecht University

Prof. dr. Femke van Wijk – Utrecht University

November 2022

UMC Utrecht, Heidelberglaan 100, 3584 CX, Utrecht

LAYMAN'S SUMMARY

Cancer is the second most common medical burden in society. It is a group of diseases that involve uncontrolled cell growth, with the potential to spread throughout the body. If left untreated and spreads, it can inhibit healthy tissues from functioning properly and will be lethal.

A tumor microenvironment consists of a local environment with cancer cells, immune cells, and supportive cells that form blood vessels or produce supportive tissue. The many elements of the tumor microenvironment that are present can negatively influence invading immune cells that are supposed to attack tumor cells. In healthy individuals, an active immune system can rid the body of external pathogens, and of abnormal cells. However, in cancer these cells escape destruction by the immune system.

T lymphocytes, a type of white blood cell, invade tumors in an effort to destroy these derailed cancer cells. In some tumors T cells, are prevented from destroying cancer cells, while in others they succeed, depending on the tumor microenvironmental effects on their invading and killing capacity.

Immunotherapy is a class of therapies that uses the immune system to eliminate cancer cells. The activity of T lymphocytes can be restored by immune checkpoint inhibitors: they block contact points on the cells that normally temper killing. Unfortunately, immune checkpoint inhibitors are like a double-edged sword: whilst some T lymphocytes' activity is restored, others become over-active thereby instigating autoimmunity. Additionally, it can be hard to predict who and how each patient will respond.

This project aims to gain an understanding of the process of changing from an active T lymphocyte to an exhausted T lymphocyte by modeling it outside the human body. Is the exhaustion process something that we can effectively model outside the human body? And can we for instance define substages and relate them to response to immune checkpoint inhibitors? This model can contribute to a better understanding of how several tumor microenvironment elements contribute to exhaustion and contribute to responses to immune checkpoint inhibitors.

For this, we used a flow cytometry panel. The technique enables a researcher to investigate the appearance of cells, based on different types of proteins that can be present on the inside or outside of the cell. Eleven different proteins were chosen to measure on the T lymphocytes based on the literature. To model the process, healthy T lymphocytes were activated in a culture dish with beads covered in activating proteins. Then, at several timepoints, we measured markers for T cell exhaustion. We observed changes in protein expression in line with some characteristics leading up to the most final stage of exhaustion. For future research there are more aspects other than cell appearance, such as their ability to excrete signaling or killing molecules, which could be measured in this model to more extensively validate our findings.

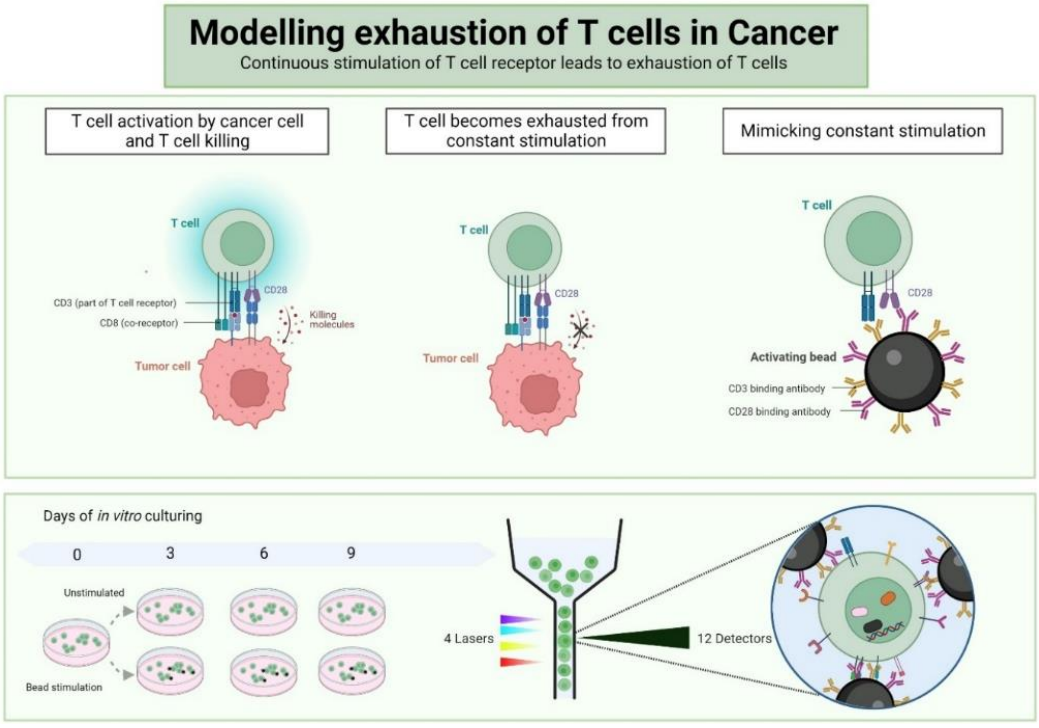

ABSTRACT

Reviving the activity of tumor-specific T lymphocytes has improved cancer treatment since the introduction of immunotherapy, specifically immune checkpoint inhibition. Nevertheless, a large number of individuals do not respond or have a long-lasting response. Tumor infiltrating T cells indeed can exhibit a wide range of dysfunctional states, referred to as exhaustion. This exhausted state is thought to be an important contributor in non-response to immune checkpoint inhibition. On top of chronic antigen stimulation, many suppressive elements present in the tumor microenvironment influence T cell progression to exhausted states. Studies in murine systems and on human tumor samples have thus far brought insight into the mechanisms inducing- and influencing progression of exhaustion in the T cells. In this study, we present a provisional human model for *in vitro* T cell exhaustion. In this model, we show upon activation with T cell receptor stimulating beads that CD8+ T cells express hallmark surface receptor PD-1 and key transcription factor TOX. Additionally, both CD4+ and CD8+ T cells express other inhibitory receptors. Furthermore, expression of Eomes is revoked upon stimulation, indicating that the T cells display intermediate substages of exhaustion. Taken together, T cell receptor stimulation with beads can partially mimic T cell exhaustion in a model which can be used and optimized to further investigate effects of the tumor microenvironment on T cell activation and exhaustion, and how this may be contributing to immunotherapy response

***Keywords**: T cell exhaustion, CD8, TCF1, TOX , immune checkpoints, immune checkpoint inhibitors, cancer*

LIST OF ABBREVIATIONS

CD – cluster of differentiation

CTLA-4 – cytotoxic T-lymphocyte associated protein 4

ICPI – immune checkpoint inhibition

IFN-γ - interferon-gamma

irAE – immune related adverse effects

LAG-3 – leukocyte activation gene 3

MDSC – myeloid-derived suppressor cells

NaHep – Sodium Heparine

PBMC – peripheral blood mononuclear cells

PD-1 – programmed death ligand 1

PHA - phytohemagglutinin

PMA - Phorbol 12-myristate 13-acetate

scRNA-seq – single cell RNA sequencing

TCR – T cell receptor

TIL – tumor infiltrating lymphocyte

TME – tumor microenvironment

Treg – regulatory T cells

INTRODUCTION

In cancer, tumors contain genetic changes resulting from DNA damage, which can be induced by a myriad of factors such as replication stress or UV radiation (1). For instance, cancer cells can produce abnormal proteins that are presented as antigens, thereby summoning an adaptive immune response (2). Frequently, this adaptive response involves T cell responses to tumor cells, and the presence of CD8+ cytotoxic T cells is a positive prognostic marker in several solid tumors, such as ovarian, colorectal, neck, bladder cancer, and melanoma (3). However, these cells may still not succeed in eradicating all cancer cells (4). In the tumor microenvironment (TME), T cells are subjected to a multitude of factors that diminish their effector functions and lead to a state called exhaustion (5).

Under the umbrella term T cell exhaustion, some general hallmarks are accepted: one very distinct characteristic of exhausted T cells is sustained upregulation of programmed cell death protein 1 (PD-1). The changed functional state of PD-1+ T cells, labeled T cell exhaustion, has been described thoroughly in the context of chronic infection with lymphocytic choriomeningitis virus (LCMV) infection in murine models (6,7). Furthermore, it is characterized by decreased cytolytic function; increased chemokine expression; persistently high levels of expression of multiple inhibitory receptors, such as PD-1, LAG3, and CTLA4; decreased (but not absent) cytokine production; reduced proliferative capacity when stimulated; an altered transcriptional program involving the transcription factor TOX; and a unique epigenetic landscape (8,9).
T cell exhaustion is mostly described in CD8+ cytotoxic T cells, but some discussion is ongoing on whether this may also occur in CD4+ T cells. They can express several immune checkpoints, decrease cytokine expression, and express the transcription factor TOX (10,11). TOX has been described in CD8+ cells to epigenetically rewire cells to an exhausted transcriptional program, with some epigenetic changes being irreversible (12–14).

It is important to discriminate between T cell anergy, senescence, and exhaustion, as they share the characteristics of decreased proliferation and production of several cytokines. Anergy occurs at the molecular level by co-stimulation-deficient T cell receptor (TCR) activation, resulting in a state that cannot surmount the required immune response for eradication of the target. For example, this leads to a decrease in IL-2 production, which is important for T cell maintenance and self-renewal. In contrast, senescence occurs when cells reach the limit of their replicative capacity owing to telomere erosion. For instance, certain cytokines such as interferon-gamma (IFN-γ), which directly inhibit telomerase, can accelerate senescence (15). This also leads to very little proliferation and defective effector functions. In contrast, exhausted T cells are activated through co-stimulation and have the capacity to be reactivated upon removal from the antigen, depending on the extent of their exhaustion (16,17).

One way to revive T cell function is by blocking the axis of PD-1 and its ligand, PD-L1, which demonstrates the relevance of this axis in early T cell exhaustion (18). As a result, antibodies targeting either PD-1 or PD-L1 have exhibited promising results in multiple cancer types (19–21).
T cells can express several different inhibitory receptors, termed immune checkpoints, which increase with the progression of exhaustion (16). Antibodies therapeutically targeting alternative immune checkpoints like CTLA-4 display synergistic effects is the clinical setting, likely targeting several T cell subsets (22).
Significant clinical results for some patients have been obtained with immune checkpoint inhibitors (ICPI) through tumor size maintenance or reduction, showing a clear advancement in patient outcomes. Nonetheless, the response rates are suboptimal, due to resistance in the targeted T cells. Patients can also experience unpredictable immune-related adverse events (irAEs). The overall incidence of severe irAEs is 20-30% with ipilimumab, which targets CTLA-4, and 10-15% for patients receiving anti-PD-1 agents. Over half of life-threatening cases occur in patients treated with combinatorial therapy (23). Ipilimumab, the first antibody approved by the FDA, can cause colitis and hypophysitis, whereas pneumonitis and thyroiditis are frequently observed when treated with nivolumab and pembrolizumab, which target PD-1 (24–27). There is great interest in predicting the response to ICPI and the development of irAEs associated with them. For instance, gut microbiome can influence the response to anti-PD-1 monotherapy regarding tumor response and irAEs (28). Next to this, tumor cell characteristics hold a relationship to response. For example, tumor mutational burden leads to a larger diversity of neoantigens presented to T cells with vice versa a high diversity of T cell receptors also being found in responders to immunotherapy (9,29,30).

The many immunosuppressive mechanisms intratumoral T cells are subjected to lead to an anticipated wide spectrum of exhausted states as a result. In the TME immunosuppressive cell populations can be present, as well certain metabolites or enzymes that repress their function, but also physiological and nutrient changes in the TME (31,32). T

cells are affected by the altered metabolism of tumor tissue, are depleted of critical nutrients, and surrounded by suppressive metabolites, like lactic acid (31–33). Immunosuppressive cells like myeloid-derived suppressor cells (MDSCs) and regulatory T cells (Tregs) can be present tumors both proximally and distally exert their effects on T cells: MDSCs can express proteins like arginase-1, oxide synthase 2, NAPDH oxidase and S100A8, whereas Tregs exert their suppression through producing cytokines like IL-10 or expressing inhibitory receptors that deprive antigen presenting cells of co-stimulatory signaling for T cells in mice (34–37).
The heterogeneity in T cell populations found in tumors may thus be a representation of T cells that are developmentally in several early to terminal stages of exhaustion (5). Combining flow cytometry to sort immune cells vs stroma from dissociated tumors, and single cell RNA sequencing (scRNA-seq), has shown that exhausted T cells are found in both responders and non-responders to ICPI, depending on how T cell exhaustion is defined (9,38,39). Imaging studies, like imaging mass cytometry and RNA scope bring insights into the significance of cell localization and interactions within the tumor microenvironment from intact tumor samples in relation to ICPI response for prognostic patient stratification. Studying these more proximal interactions *in vitro* may shine light on mechanisms contributing to the heterogenous pool of exhausted T cells contributing to ICPI response, but also additional opportunities to intervene.

More recently, developmental stages of exhaustion in CD8+ T cells have been described with transcription factors TCF-1 (encoded by *Tcf7*), T-bet, Eomes and TOX as regulators of developmental hierarchy (16). In mice, intermediate exhausted T cells (Tex^{int}) were blood-accessible, proliferative, showed increased effector biology, and clonally expanded upon blockage of PD-1/PD-L1 signaling **(Figure 1).** Blood accessibility was determined based on staining of vasculature in mouse tumors and revealed limited locations of the subsets. Regarding proliferation, this was assessed *ex vivo* after sorting for delineating marker Ly108 (murine homolog of human Slamf6) and CD69. Increased effector biology was determined by comparing the excretion of TNF-α and IFN-γ (16). Similar patterns in human were found in human melanoma samples: distribution between subsets, proliferative capacity based on Ki67 expression, expression of the regulating transcription factors TCF-1, T-bet, Eomes and TOX, and lastly cytolytic ability *ex vivo* (16). The developmental transition from intermediate to terminally exhausted is intriguing to study in context of the functional implication and potential intervention. Understanding how the tumor microenvironment contributes to T cell transitioning to a stage in which exhaustion may not be reversed, may highlight predictive factors of ICPI response for patient stratification or bring insight to further opportunities of intervention.

To dynamically study the effects of extrinsic factors on T cell exhaustion, mouse models have been used. Human samples are dependent on clinically obtained tumor tissue, of which tumor infiltrating lymphocytes (TILs) derived from tumor tissue. Adhering to the 3 Rs of refinement, reduction and replacement, establishing an *in vitro* human model would refine the system more closely to the organism of study, reduces costs, reduce time and limits the ethical considerations tied to *in vivo* models. Moreover, limited availability of human clinical tumor samples imposes a challenge to study T cell exhaustion. Experimental exploration is terminal to samples, requiring sufficient available input. To add, not all samples may be suitable to study the full spectrum of T cell exhaustion. To overcome this, modelling T cell exhaustion with T cells derived from healthy individuals would allow for further examination of T cell exhaustion with applications of ICPI in co-cultures.

In this project, we aim to establish an *in vitro* model of CD8+ T cell exhaustion (**Figure 2A**). This is done by isolation of peripheral blood mononuclear cells (PBMC) from healthy human donors. Following isolation, pan-T cells are separated and cultured *in vitro* under conditions of chronic antigen exposure mimicked by TCR- and co-stimulation to induce several hallmarks of exhaustion, in comparison to non-stimulated T cells in culture. Corresponding to this model, a 12-color flow cytometry panel was designed to measure markers that relate to T cell exhaustion, of which several discussed above (**Figure 2B**).To test suitability of the system, immunophenotyping of cells was accomplished by a flow cytometry panel designed for this study. We investigated if intermediate to terminal exhausted stages in the developmental model of Beltra et al., could be recapitulated within this model. We found that earlier stages of CD8+ T cell exhaustion, respectively Tex^{prog1} and Tex^{prog2} could be reached. Although requiring optimization and further characterization, such a model could be applied to test other elements in the tumor microenvironment their contribution to progression to Tex^{int} and Tex^{term}. This could then be combined with testing the potential of ICPI, with the objective of T cell exhaustion substage reversion and elevated killing through killing assays, also in presence of a co-culture (16). This could improve prediction of ICPI response.

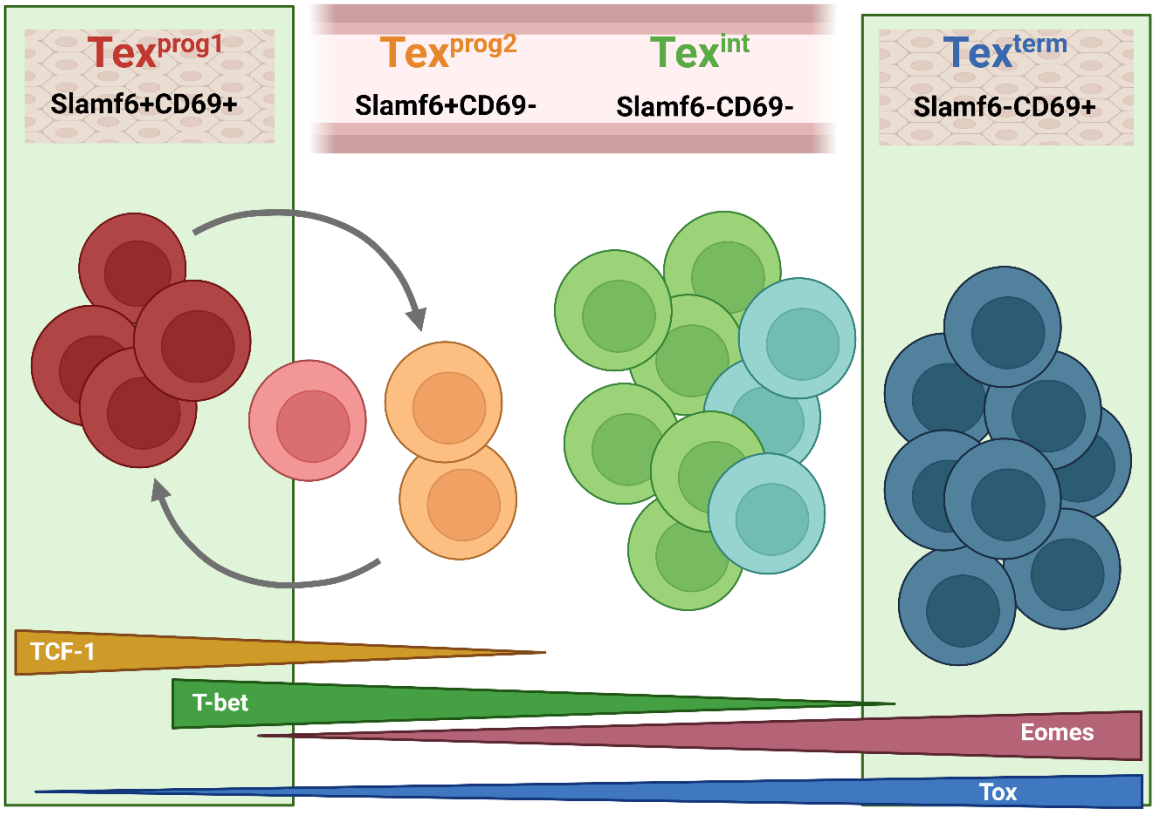

Fig. 1 Developmental stages of T cell exhaustion in a murine system.
Two tissue-restricted and blood-accessible TCF-1+ progenitor subsets were defined that gradually lost TCF-1 as it diverged into a third intermediate Tex subset (Tex^{int}). Eventually evolving into a fourth, terminally exhausted subset (Tex^{term}). An interplay between TCF1, T-bet, and Eomes control the mechanisms causing subset transitions. Tex^{int} temporarily restores effector biology and clonally expands upon PD-L1 blockade. Figure adapted from Beltra et al., (16)

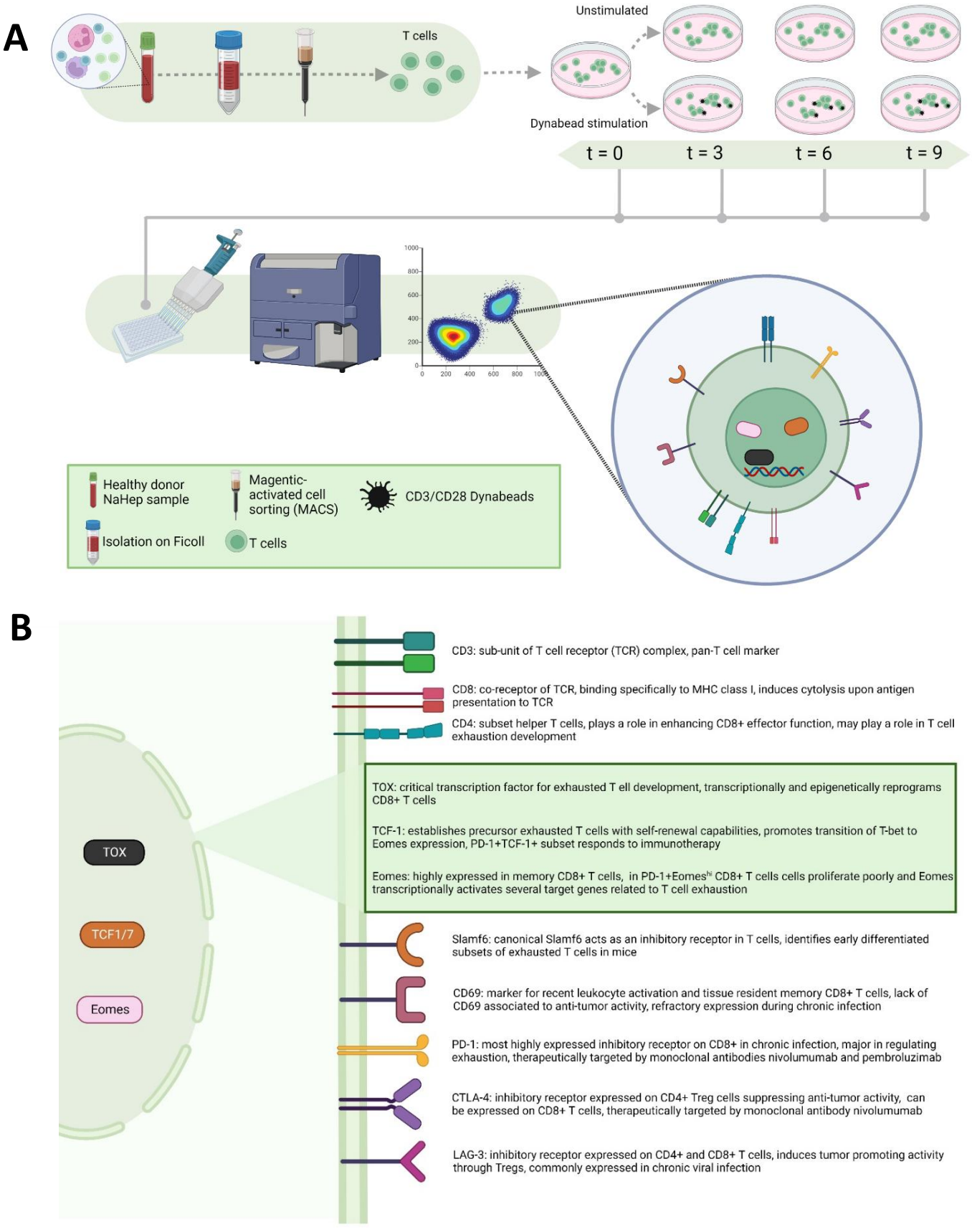

Fig. 2 Study design
A) Overview of methods. T cells were isolated from whole blood using Ficoll isolation and MACS. Next, T cells were cultured in presence of CD3/CD28 beads to mimic chronic antigen stimulation. At subsequent culturing timepoints, cells were collected and stained with a flow cytometry panel measuring markers relevant to T cell exhaustion. B) T cell exhaustion flow cytometry panel. Abbreviations: CD = cluster of differentiation; TCR: T cell receptor. Sources from text: CD3 (40,41); CD8 (42); CD4 (43,44), TOX (12); TCF-1 (45,46); Eomes (47,48); Slamf6(16,49,50); CD69 (51–53); PD-1 (54–58); CTLA-4 (59,60); LAG-3 (41,61)

MATERIALS AND METHODS

PBMC ISOLATION

Human adult PBMCs were isolated from blood from healthy donors (NaHep), by means of density gradient centrifugation at 2300 rpm at room temperature with the separating solution Ficoll®Paque Plus (Sigma-Aldrich, St Louis, MO, USA) for 30 min with the brakes off. The layer containing PBMCs was collected and washed twice with medium: RPMI1640 (Capricorn Scientific, Epsdorfergrund, Germany) with 10% fetal bovine serum (Bodinco BV, Alkmaar, Netherlands), 1% penicillin/streptomycin (Sigma-Aldrich, St Louis, MO, USA) and 1% L-glutamine (Sigma-Aldrich, St Louis, MO, USA). The two more centrifugation steps were performed at 1500 rpm for 10 min. The cell pellet was resuspended in 10 mL medium, then manually counted using Türk Liquid (Merck Millkpore, Burlington, MA, USA) and a hemacytometer. Cells were left in medium or centrifuged at 1500 rpm for 10 min and resuspended in cryo-medium: fetal bovine serum (Bodinco BV, Alkmaar, Netherlands) + 10% dimethyl sulfoxide (Merck, Kenilworth, NJ, USA). For further cell separation, PBMCs were washed at 1500 rpm for 10 min, and resuspended in its designated buffer. Information about donors can be found in the addendum (**S1**).

CELL SEPARATION

Pan-cells were separated from the PBMCs by means of magnetic-activated cell sorting (MACS) using the pan-T cell isolation kit (Miltenyi Biotec, Bergisch Gladbach, Germany) according to the manufacturers' instructions. This kit was combined with a MiniMACS™ Separator and MS Columns, and cell amounts were adjusted according to the manufacturers' instructions. T cells were counted manually and tested for viability using Trypan Blue 0.4% (Invitrogen, Waltham, MA, USA).

CELL CULTURE

pan-T cells, enriched from PBMCs. 0.5 – 2 x 10^6 T cells were plated at a concentration of 0.5-1.0 x 10^6 T cells / mL in RPMI1640 (Capricorn Scientific, Epsdorfergrund, Germany) supplemented with 10% fetal bovine serum (Bodinco BV, Alkmaar, Netherlands), 1% penicillin/streptomycin (Sigma-Aldrich, St Louis, MO, USA), 1% L-glutamine 1% L-glutamine (Sigma-Aldrich, St Louis, MO, USA) and 30 U/mL IL-2 (Immunotools, Frisoythe, Germany) in a 24-well plate. Cells were stimulated with T-Activator CD3/CD28 Dynabeads® (Life Technologies, Carlsbad, USA). Every 72h, cells were manually counted with Trypan Blue 0.4% (Invitrogen, Waltham, MA, USA) and a hemacytometer. Cell washed, and stimulated with fresh Dynabeads®, depending on cell count for recovering the recommended 1:1 cell to bead ratio. For marker controls, cells were stimulated with 5 mg/mL PHA (Oxoid BV, Landsmeer, Netherlands) for 3 days. After a round of cell stimulation, cells were counted and cultured another round or employed in flow cytometric analysis.

CELL PREPERATION

For a negative expression control HEK293T cells were obtained (gift from in-house group). To acquire a single cell suspension, cells were trypsinized (Sigma-Aldrich, St Louis, MO, USA) for 5 to 7 minutes. Using PBS, cells were taken up and washed twice by centrifuging for 5 min at 1200 rpm. Cells were then resuspended in PBS and counted using Türk Liquid (Merck Millkpore, Burlington, MA, USA) and a hemacytometer. The cells were then employed in flow cytometric staining.

FLOW CYTOMETRIC STAINING

After every round of culture with beads, samples were first stained with a LIVE/DEAD nIR 780 stains (Thermo Fisher Scientific, Waltham, MA, USA) according to manufacturer's instructions. After washing, cells were stained for characterization by flow cytometry using antibodies specific for CD3, CD4, CD8, PD-1, CTLA-4, LAG-3, CD69 (all from Biolegend, San Diego, CA, USA), TCF1/7 (BD Biosciences San Jose, CA, USA), Slamf6 (R&D Systems, Minneapolis, MN, USA), TOX (Miltenyi Biotec, Bergisch Gladbach, Germany) and EOMES (Thermo Fisher Scientific, Waltham, MA, USA). Prior to fixation, samples were resuspended every 10 min in all steps to avoid clumping in adherent cell samples. Before fixation, cells were stained for 20 minutes in the dark in FACS Buffer (PBS + 0.1% BSA + 0.05% NaN_3) in a 96-wells U-bottom plate (Corning® Falcon, Corning, NY, USA). Further fixation and staining of the cells with intracellular antibodies was performed using the eBioscience™ FOXP3 / Transcription Factor Staining Buffer Set (Thermo Fisher Scientific, Waltham, MA, USA). After fixing/permeabilizing for 30 minutes in the dark, cells were washed three times with 100 µl of permeabilization buffer. Antibodies to intracellular and nuclear markers were added in 50 µl of permeabilization buffer, incubated at RT for 30 min in the dark, and then washed three times with 100 µl of

permeabilization buffer. Finally, cells were resuspended in FACS Buffer (PBS + 1% BSA + 2 mM EDTA + NaN_3) and transferred to tubes before flow acquisition. Samples were measured, at a minimum of 15.000 events per tube, with the BD LSRFortessa (BD Biosciences, San Jose, CA, USA).

DATA ANALYSIS

Flow cytometry analysis was performed with Cytobank software (Beckman Coulter, Brea, CA, USA). Figures were created with GraphPad Prism V8 (San Diego, CA, USA).

For key resources table, please refer to the addendum (**S2**)

RESULTS

A T cell exhaustion flow cytometry panel was optimized, tested and validated

For panel validation, antibodies were first tested and titrated to optimal concentrations on PBMC fractions. Optimal concentrations were determined based on if it was possible to discriminate between a negative and positive population. In the samples, debris and double events were gated out first. α-CD69-BV510 was tested using a PHA positive control and titrated to 1:400 (**Figure 3A**). α-CD3-PerCP was tested and titrated to 1:400 (**Figure 3B**). α-CD4-BV605 was tested and titrated to 1:100 (**Figure 3C**). In addition, this concentration had the highest staining index (SI)for CD4. The SI is defined as $SI = \frac{meanPos - meanNeg}{2SDneg}$ (62). It was decided to retain this staining concentration for further experiments but in the following tests do away with the SI for more sustainable use of reagents, as for we could still delineate positive and negative populations at lower concentrations even though a higher concentration gave a higher staining index. α-CD8-BV711 was tested and titrated to 1:400 (**Figure 3D**). We tested several antibodies making use of a positive control, under the suggestion of the manufacturer. Several stains were tested for the option to use 3-day PHA stimulation (5 mg/mL) as a positive control for T cell activation. All markers showed positive staining upon stimulation at their respective concentrations (**Figure 3E**). Stainings were re-tested at their respective concentrations, in the definite choice of buffer: FOXP3 Transcription Buffer Staining kit (**Figure 3F**). Use of this buffer enabled staining of transcription factors and did not affect signal from other stainings. α-Slamf6-APC was tested and titrated to 1:400 (**Figure 3G**). In comparison to 1:50, 71% of cells could still be considered positive at 1:100, when 86% was positive at 1:50 dilution. α-Eomes-PE-Cy7 was tested and titrated to 1:100 (**Figure 3H**). At this concentration, it was possible to distinguish between a lower and higher level of Eomes expression. α-TOX-PE was tested, in co-stain with CD4, and titrated to 1:50 (**Figure 3I**). At this concentration, it was possible to distinguish two TOX+ populations, which decreased through dilution. α-LAG-3-BV650 was tested and titrated to 1:400 (**Figure 3J**). α-TCF-1-HorizonRed718 was tested and titrated, to 1:50 dilution (**Figure 3K**). At this concentration, positive staining was observed overall and enabled discrimination between an intermediate and higher TCF-1 population. LIVE/DEAD stain nIR 780 stained cells and could discriminate viable cells (**Figure 3L**). α-PD-1-FITC was tested and titrated to 1:50 dilution (**Figure 3M**). Dilutions beyond this reduced staining significantly, so 1:50 was adhered to. α-CTLA-4-BV421 was tested and titrated to 1:400 dilution (**Figure 3N**). This allowed for discrimination between a negative and positive population. After single stain titrations, we proceeded to the full panel staining stained on PHA-stimulated PBMC. These samples were used to establish compensation for spectral overlap, which is critical for interpretation of multi-marker flow cytometry results (**S3**). Panel configuration with our equipment can be found in the addendum (**S4**).

For the staining protocol, we used 100.000-500.000 cells per well in a 96-wells plate. Depending on the amount of sample available from our culture system we opted for highest possible number of cells. This was done as the protocol from the LIVE/DEAD stain and the FOXP3 kit combined included many washing steps. This ensured sufficient cells were present for flow cytometric measurements. As previously used protocols were not compatible with all antibodies, we switched to the FOXP3 kit. Therefore, several stains were also retested in the FOXP3 kit protocol for compatibility (**Figure 3F**).

The full panel was stained on PHA stimulated PBMCs and compensated comparing single stains. However, some markers showed strange staining pattern with a positive and negative population in a single channel with a single stain, indicating that during the staining process some samples have overflown (**S3C**; **S3D**; **S3F**; **S3G**; **S3H**; **S3I**).

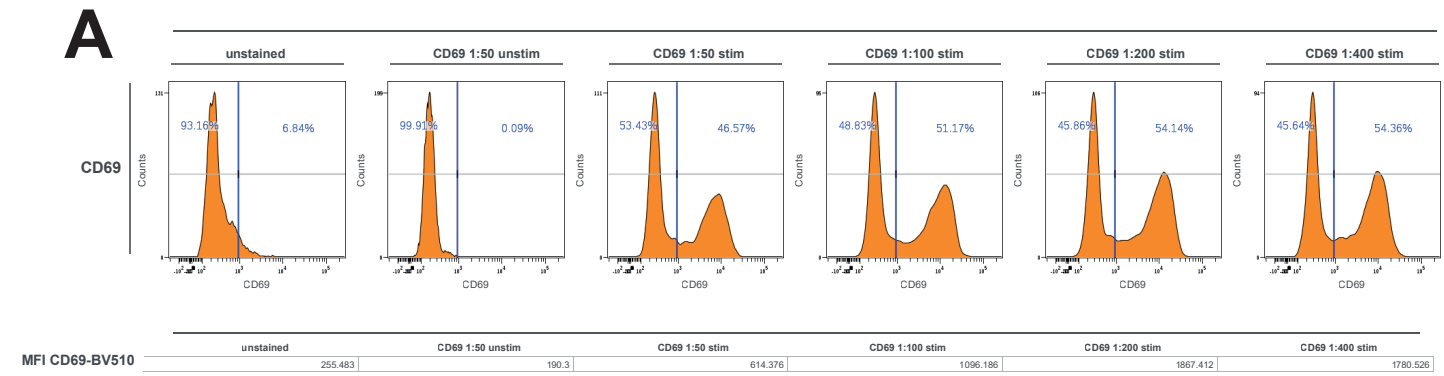

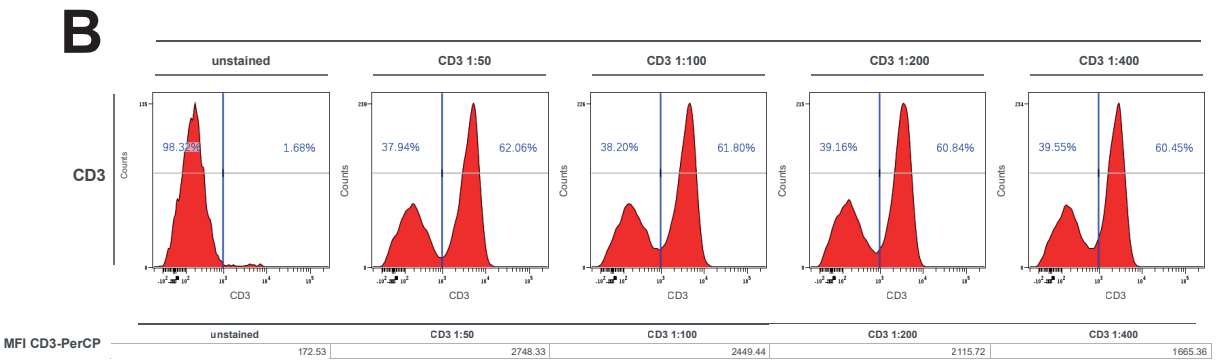

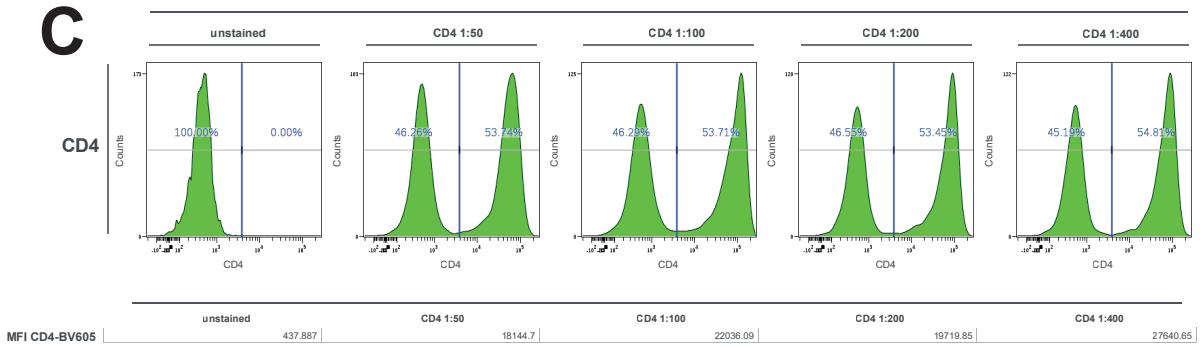

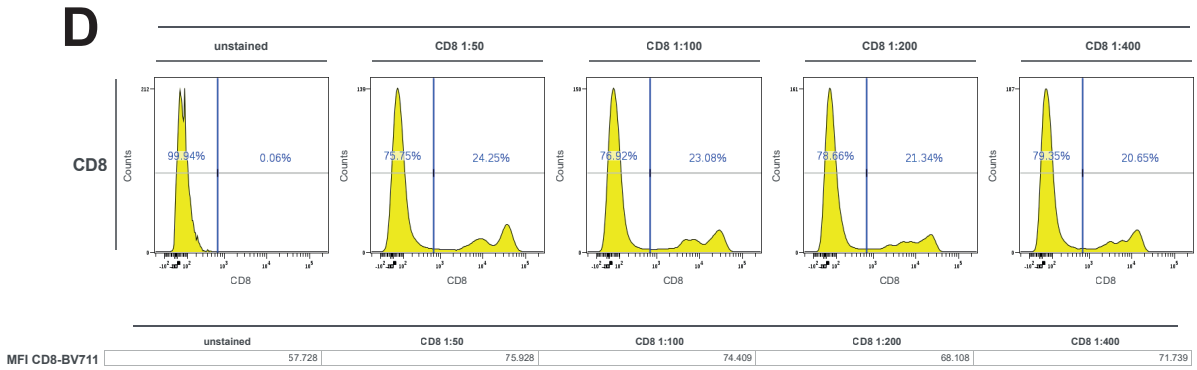

Fig. 3 T cell exhaustion panel antibody testing and titration.
Staining was performed using the FOXP3 Transcription Buffer Set (eBioscience), unless indicated otherwise. Stimulated conditions are 3-day PHA stimulation (5 mg/mL), unless indicated otherwise. MFI: Median Fluorescent Intensity. MFI below histograms. A, B, C and D were fixed with 2% PFA for 15 minutes prior to surface staining. A and F used PMA/ionomycin (20 ng/mL; 1 uM) as a positive control. A was stimulated for 6h and F for 4h. A) CD69-BV510 single stain titration series. control. Antibody be diluted up to 1:400. B) CD3-PerCP single stain titration series. Antibody can be diluted up to 1:400. C) CD4-BV605 single stain titration series. Antibody can be diluted up to 1:400. D) CD8-BV711 single stain titration series. Antibody can be diluted up to 1:400.
(Figure continues on next page)

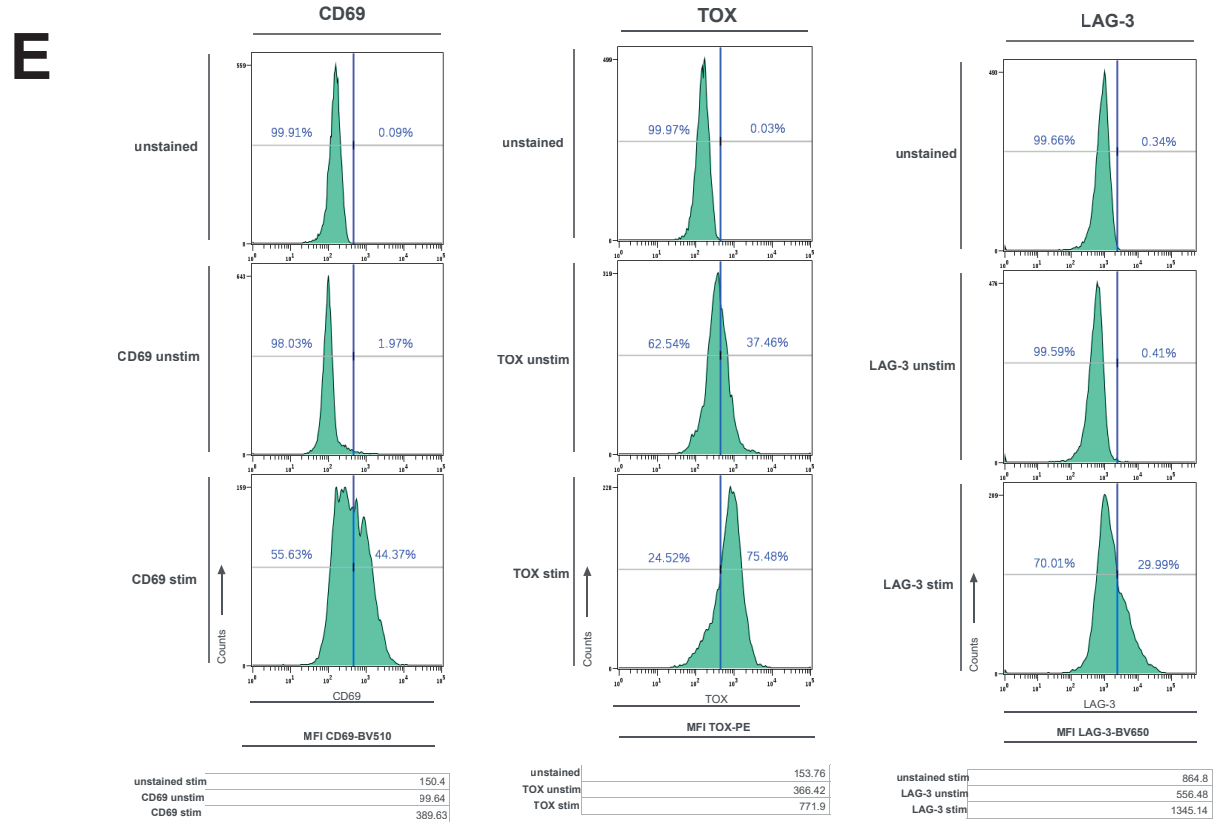

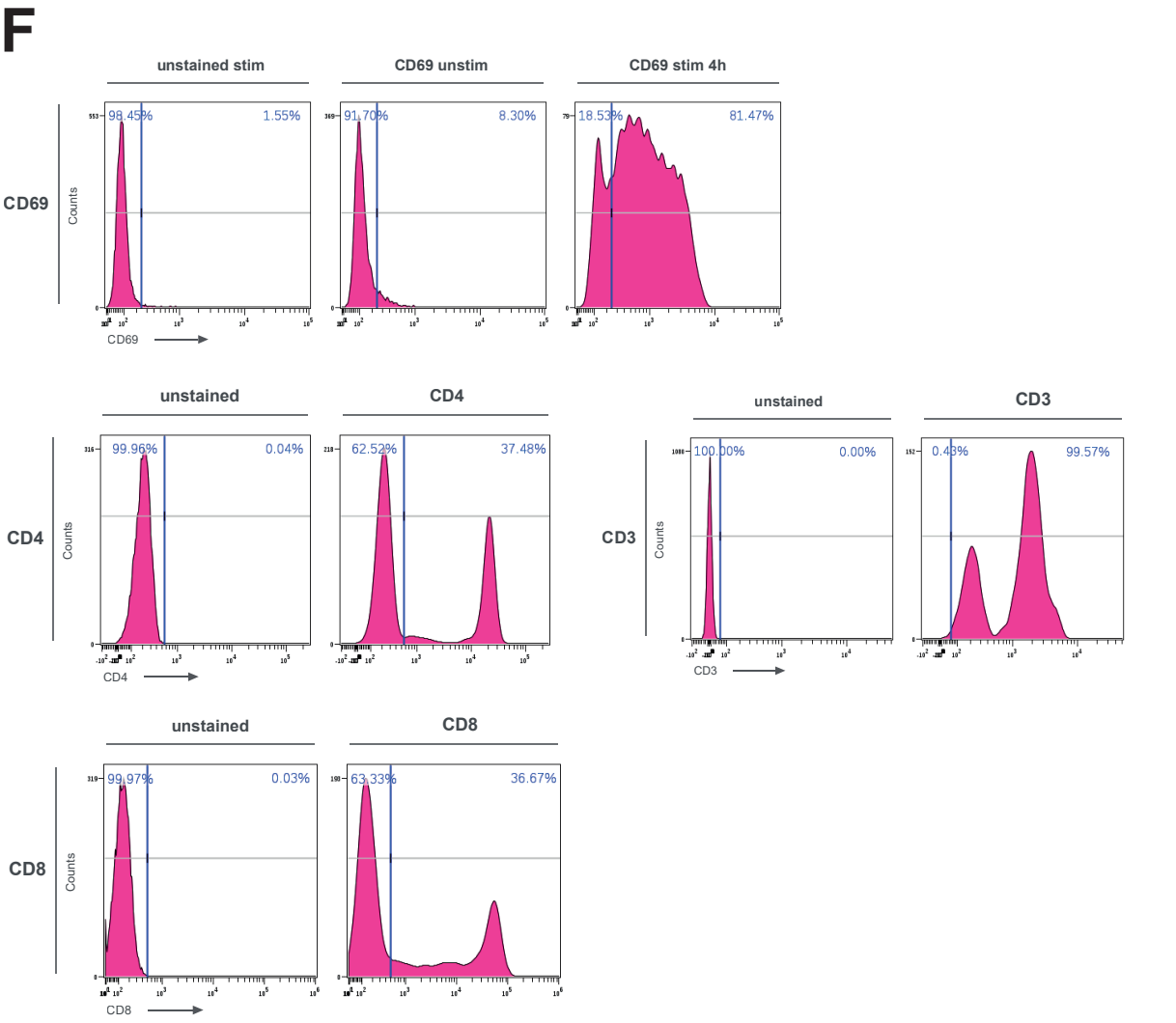

Fig. 3 T cell exhaustion panel antibody testing and titration (continued)
Staining was performed using the Foxp3 Transcription Buffer Set (eBioscience), unless indicated otherwise. Stimulated conditions are 3-day PHA stimulation (5 mg/mL), unless indicated otherwise. MFI: Median Fluorescent Intensity. A and F used PMA/ionomycin (20 ng/mL; 1 uM) as a positive control. A was stimulated for 6h and F for 4h. MFI below histograms. E) CD69, LAG-3 and TOX tested in 3-day PHA stimulation (5 mg/mL) for use as positive control. F) CD69, CD3, CD4, CD8 were re-tested in established dilutions with Foxp3 Transcription Buffer Kit (eBioscience). CD69 was stimulated with PMA/ionomycin for 4h as a positive control.
(Figure continues on next page)

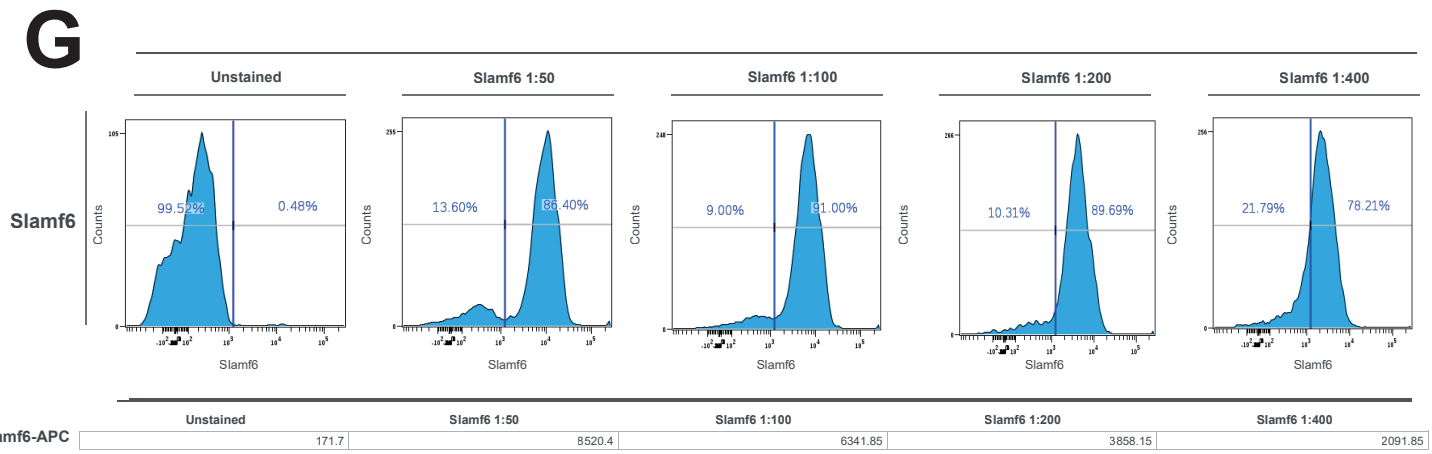

MFI Slamf6-APC	Unstained	Slamf6 1:50	Slamf6 1:100	Slamf6 1:200	Slamf6 1:400
	171.7	8520.4	6341.85	3858.15	2091.85

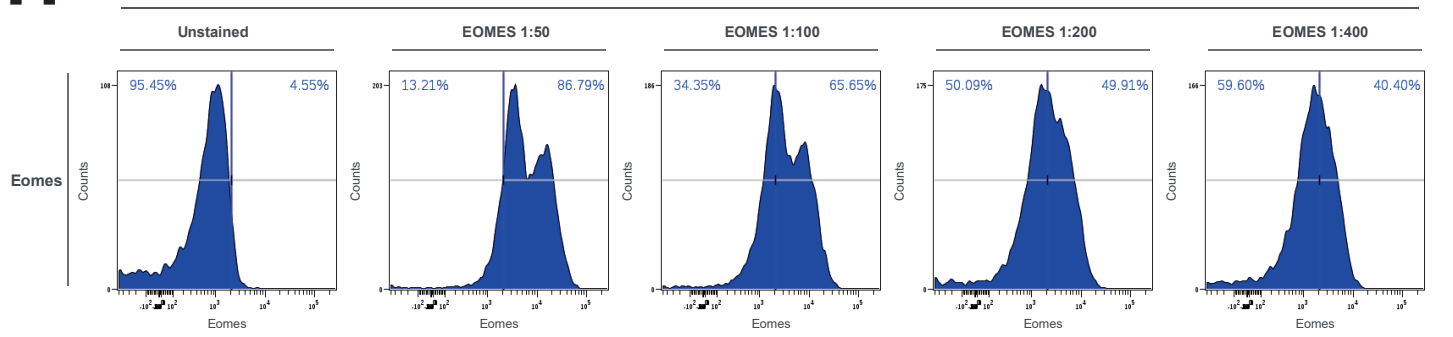

MFI Eomes-PE-Cy7	Unstained	EOMES 1:50	EOMES 1:100	EOMES 1:200	EOMES 1:400
	786.78	5277.75	3057.22	2089.4	1676.48

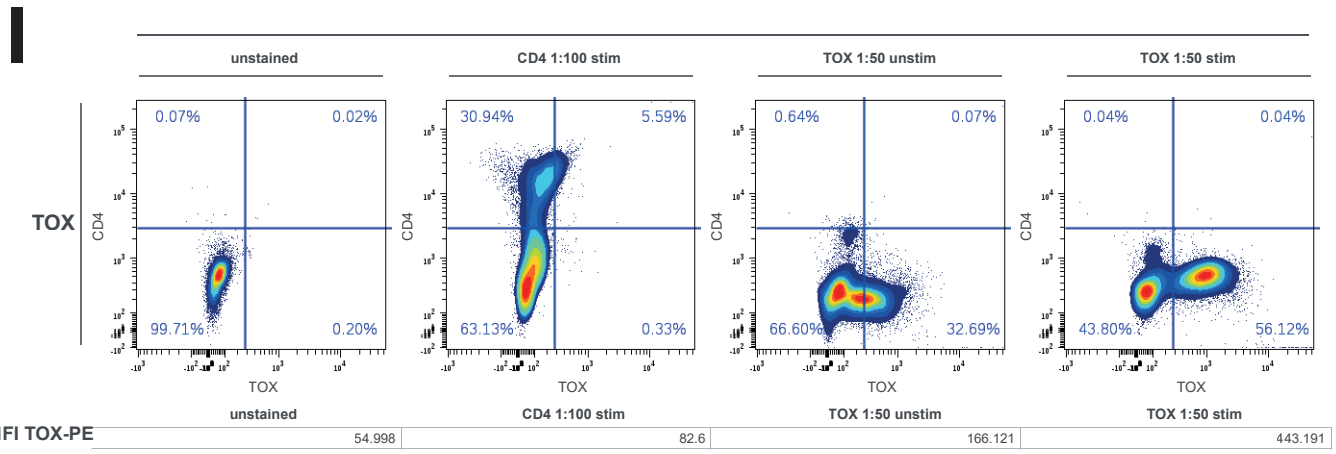

MFI TOX-PE	unstained	CD4 1:100 stim	TOX 1:50 unstim	TOX 1:50 stim
	54.998	82.6	166.121	443.191

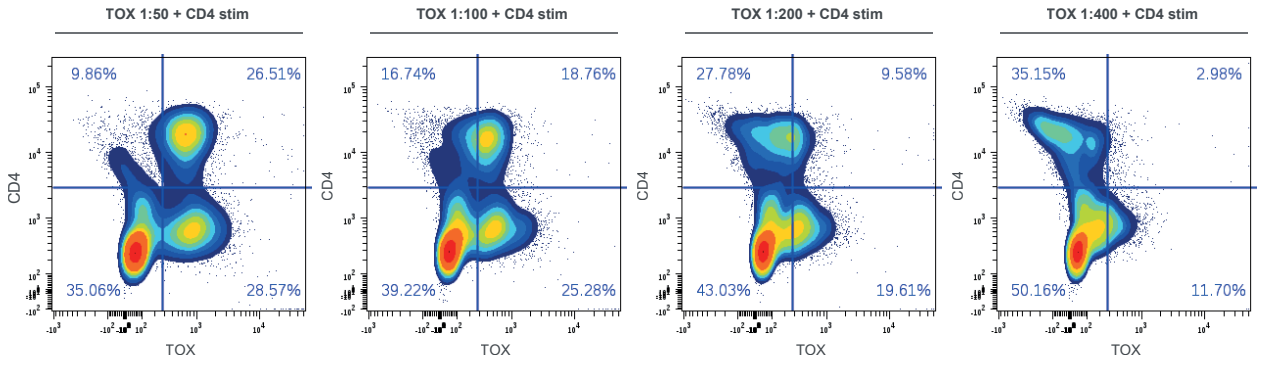

MFI TOX-PE	TOX 1:50 + CD4 stim	TOX 1:100 + CD4 stim	TOX 1:200 + CD4 stim	TOX 1:400 + CD4 stim
	375.426	208.886	121.628	67.816

Fig. 3 T cell exhaustion panel antibody testing and titration.
Staining was performed using the Foxp3 Transcription Buffer Set (eBioscience), unless indicated otherwise. Stimulated conditions are 3-day PHA stimulation (5 mg/mL), unless indicated otherwise. MFI: Median Fluorescent Intensity. MFI below histograms/plots. G) Slamf6-APC single stain titration series. Antibody can be diluted up to 1:400. H) Eomes-PE-Cy7 single stain titration series. Antibody can be diluted up to 1:100. I) Tox-PE titration series in co-stain with CD4-BV605.
(Figure continues on next page)

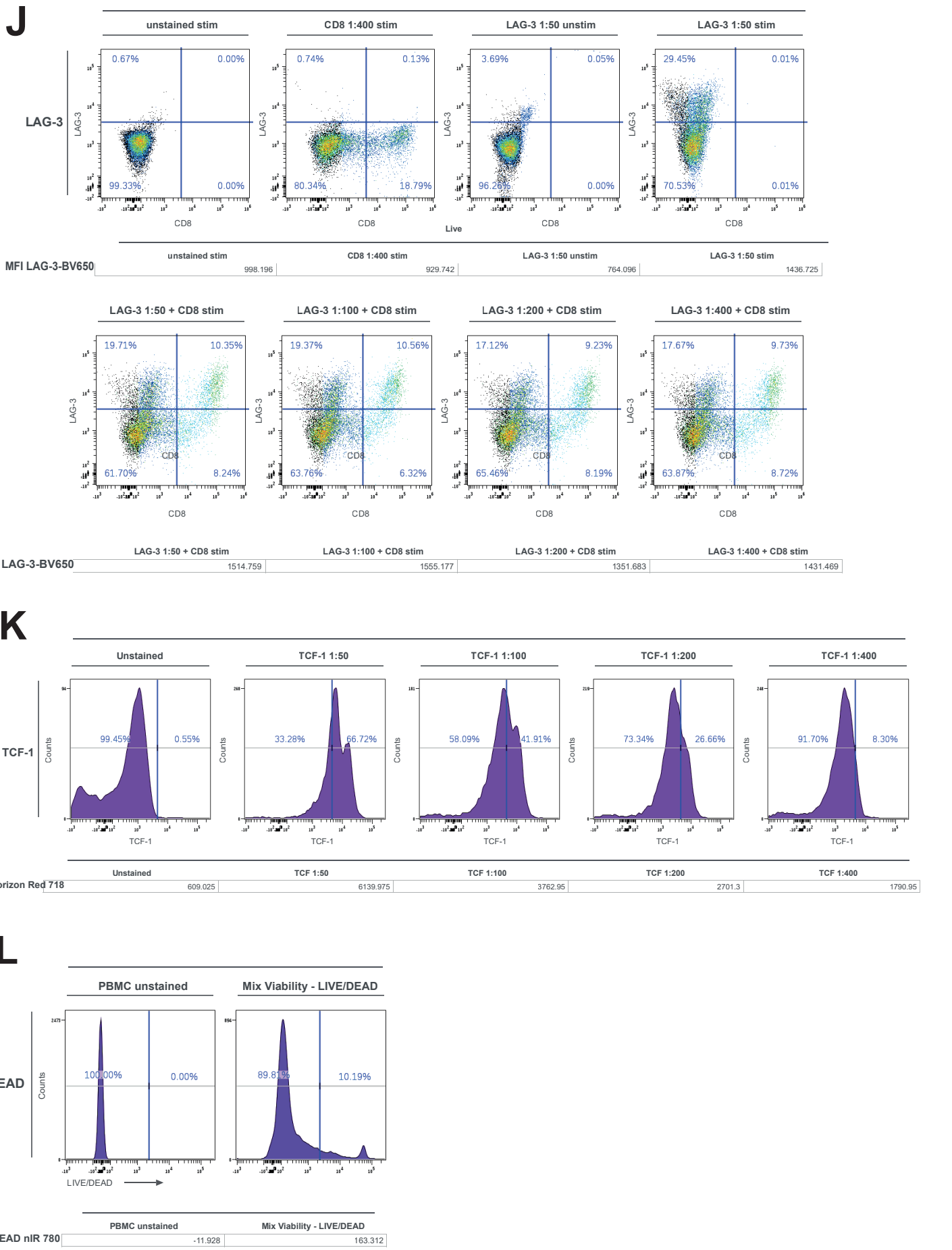

Fig. 3 T cell exhaustion panel antibody testing and titration (continued)

Staining was performed using the FOXP3 Transcription Buffer Set (eBioscience), unless indicated otherwise. Stimulated conditions are 3-day PHA stimulation (5 mg/mL), unless indicated otherwise. MFI: Median Fluorescent Intensity. MFI below histograms. J) LAG-3-BV650 single stain titration series. Antibody can be diluted up to 1:400. K) TCF1/7-Horizon Red 718 single stain titration series. Antibody can be diluted up to 1:50. L) LIVE/DEAD nIR 780 test. PMBCs were compromised using 90% ethanol and mixed with stained intact PBMCs.

(Figure continues on next page)

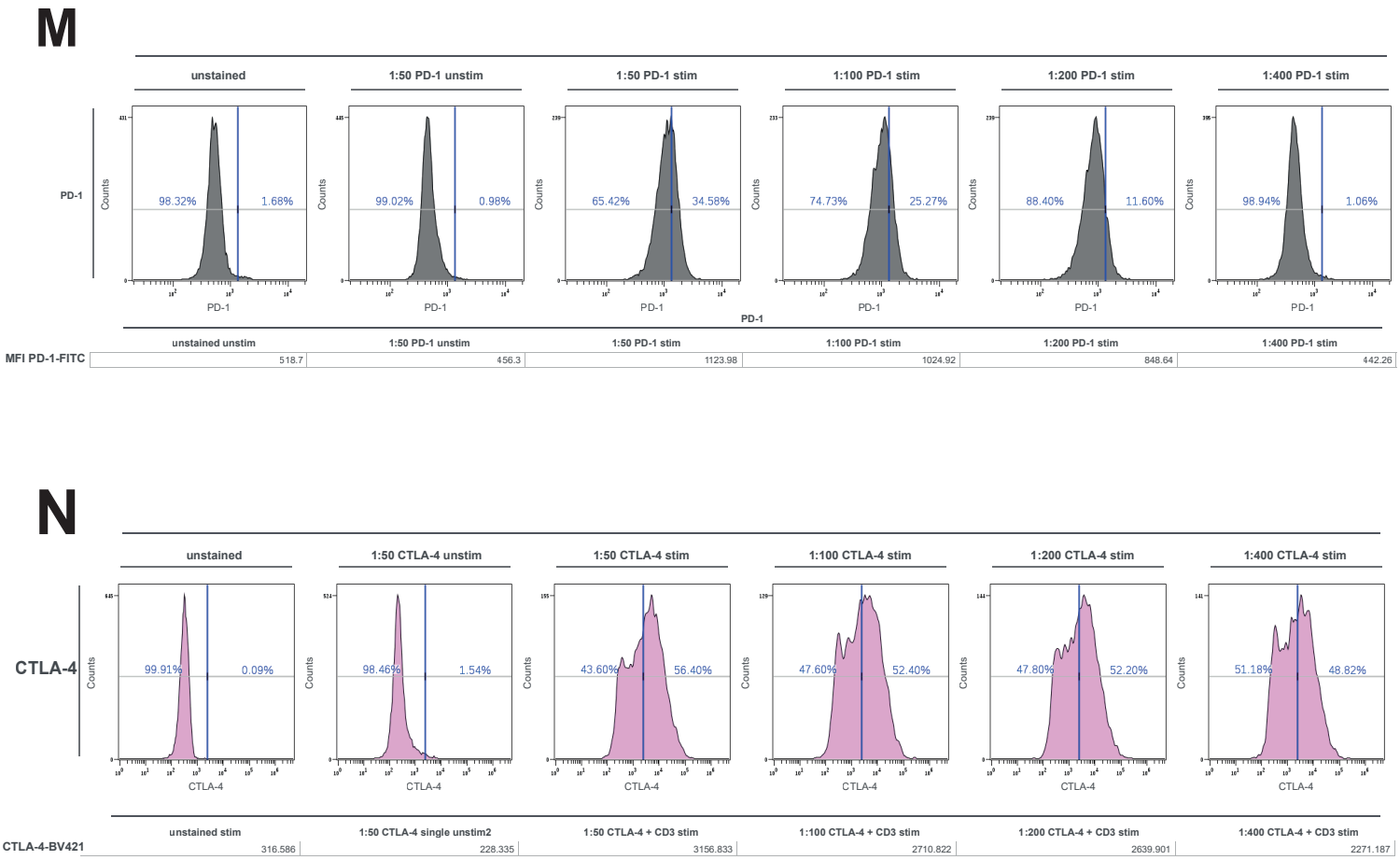

Fig. 3 T cell exhaustion panel antibody testing and titration (continued)

Staining was performed using the FOXP3 Transcription Buffer Set (eBioscience), unless indicated otherwise. Stimulated conditions are 3-day PHA stimulation (5 mg/mL), unless indicated otherwise. MFI: Median Fluorescent Intensity. MFI below histograms. M) PD-1-FITC single stain titration series. Antibody can be diluted up to 1:50. N) CTLA-3-BV421 single stain titration series. Antibody can be diluted up to 1:400.

Analysis strategy for measuring T cell exhaustion using a flow cytometry panel

For analysis of T cell exhaustion markers and T cell subsets, we designed an appropriate gating strategy (**Figure 4**). First, cells were gated depending on size and thereby also excluding debris (**Figure 4A**). Only single cell measurement events were included (**Figure 4B**). Viable cells were selected based on the LIVE/DEAD stain, selecting for the negative signal (**Figure 4C**). A CD8+ gate based on CD3+ and CD8+ was used to select the cytotoxic T cells, which are of main interest in the population, and separate them from the CD8- T cells in the culture (**Figure 4D**). This was followed by a selection based on PD-1 expression, as this is a hallmark of T cell exhaustion and a target of ICPI (**Figure 4E**). TOX expression was assessed after gating for our main interest T cells, CD8+ (**Figure 4F**). Next, within the CD8+PD-1 T cells, we established gates for expression of other inhibitory receptors CTLA-4, an ICPI target, and LAG-3, combined with being CD3+. Continuing in the PD-1+CD8+ gate, we gated separately for markers that could delineate exhaustion stages. Together with CD3+ we set gates for CTLA-4, LAG-3, TCF-1, Slamf6, CD69 and Eomes (**Figure 4G**). As CD4+ T cells make up a substantial amount of CD3+ cells in the culture system and may also display exhaustion characteristics, they are separately gated within the CD3+ population, and interrogated further with the same gates set after the CD8+ T cell population (**Figure 4H**). As no full panel stained PBMC control was present in the dataset, coordinates of x- and y-axis for threshold determination of the gate was set on single stains. All single stains can be observed in their respective channel within the supplementary data (**S3**). To negatively control marker expression (apart from TCF-1), HEK293T cells were used with separate gates (**S5**).

Exhaustion induction in vitro in T cells displays hallmark proteins PD-1 and TOX

We investigated whether culturing T cells with CD3/CD28 beads induced the expression of the inhibitory receptor PD-1, which is the first upregulated inhibitory receptor upon activation, and critical exhaustion transcription factor TOX, which can epigenetically transform T cell through to terminal exhaustion. TCR and co-stimulation was compared to unstimulated, and thus mostly naïve T cells, to see whether keeping the T cells in culture *in vitro* would also affect expression of these markers (**Figure 5**). Upon stimulation, CD8+ T cells slightly increased expression of PD-1 (**Figure 5A, 5B and 5C**) compared to the unstimulated baseline (t = 0 days). In CD4+ T cells we also saw and increase of PD-1 expression upon stimulation, which was more pronounced for these cells compared to CD8+ (**Figure 5F, 5G and 5H**).

TOX expression in CD8+ T cells increased upon culturing with beads compared to baseline day 0, which can be seen in the increased fraction of TOX+ cells and slight increase in MFI. TOX expression did not change over time when T cells were kept in culture but not stimulated (**Figure 5A, 5D and 5E**). In CD4+ T cells, TOX expression increased upon culturing with beads comparing it to day 0, which can be seen in the increased fraction of TOX+ cells and slight increase in MFI (**Figure 5A, 5I, 5J**). TOX expression did not change over time when T cells were kept in culture but not stimulated. The rise in TOX was more pronounced for CD4+ T cells, compared to CD8 (**Figure 5D, 5E, 5I and 5J**).

T cells in culture express inhibitory immune checkpoints LAG-3 and CTLA-4

We then assessed whether T cells increase their expression of other inhibitory receptors, next to PD-1, upon culturing with CD3/CD28 beads. We included populations that also contain PD-1- T cells, as PD-1 expression is an important hallmark, but not decree of T cell exhaustion. LAG-3 expression rose mostly for the CD8+ T cell population and in PD-1+CD8+ T cells. (**Figure 6A**). This was not enriched for PD-1+CD8+ stimulated T cells specifically, compared to only CD8+ stimulated T cells (**Figure 6B and 6C**). CTLA-4 expression rose in both CD8+ and in PD-1+CD8+ populations upon stimulation in culture, compared to the unstimulated condition (**Figure 6G**). CTLA-4 expression rose upon stimulation in CD8+ T cells and was higher in also PD-1+CD8+ T cells (**Figure 6H**). Median expression was the highest in PD-1+CD8+ T cells, and after this CD8+ T cells. Expression peaked at 6 days and dropped the following days (**Figure 6I**).

As the presence of inhibitory receptors on CD4+ T cells can also indirectly affect readouts from co-culture experiments and there is ongoing debate on the existence of CD4+ T cell exhaustion, we sought to query their expression on the CD4+ population. LAG-3 expression was also seen in the CD4+ population, although this was less compared to CD8+ T cells (**Figure 6C, 6D, 6E and 6F**). CTLA-4 expression rose in the CD4+ population upon stimulation in culture, compared to the unstimulated condition (**Figure 6J**). A larger fraction of CD4+ T cells were CTLA-4+ (**Figure 6K**) compared to unstimulated cells, and saw a larger increase compared to CD8+ populations (**Figure 6H**). Median expression was the highest in CD4+ T cells, compared to CD8+ populations. Expression peaked at 6 days and dropped the following days (**Figure 6L**).

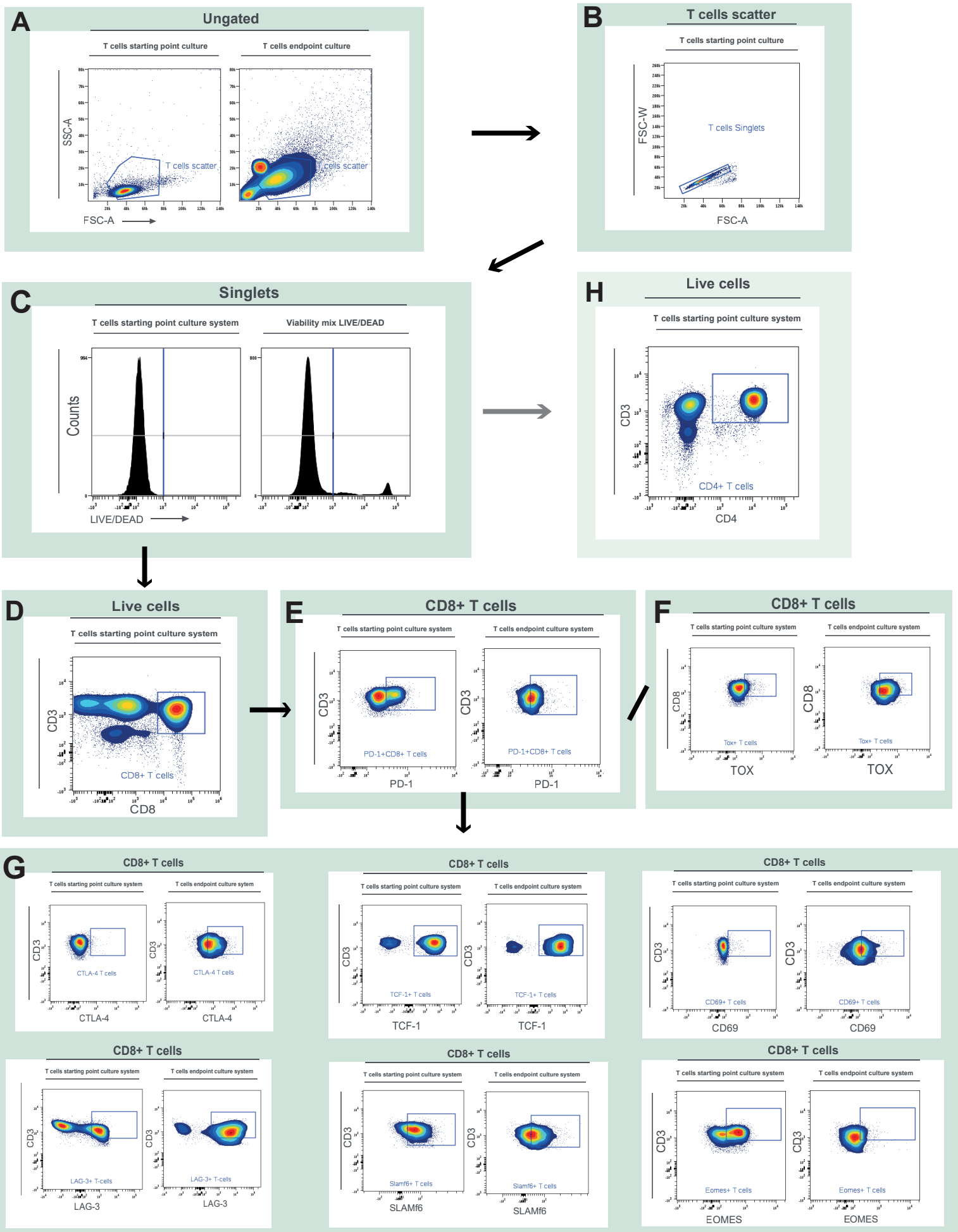

Fig. 4 Flow cytometry gating strategies for immunophenotyping of an *in vitro* model of T cell exhaustion.
This figure shows the standardized gating strategy used for the flow cytometry panel. A) Mononuclear cells (excluding debris (FSC-low/SSC-low)). B) Single lymphocytes (excluding doublets). C) Viable lymphocytes (excluding dead cells)
D) CD8+ cytotoxic T cells (CD3+CD8+). E) PD-1+ T cells (CD3+PD-1+). F) TOX+ T cells (CD3+TOX+). G) Inhibitory receptors and markers for exhaustion substage in T cells (CD3+/_). H) CD4+ T cells (CD3+CD4+), for further characterization of T cells present in the human *in vitro* model of T cell exhaustion.

Abbreviations: FSC (forward scatter), SSC (side scatter).

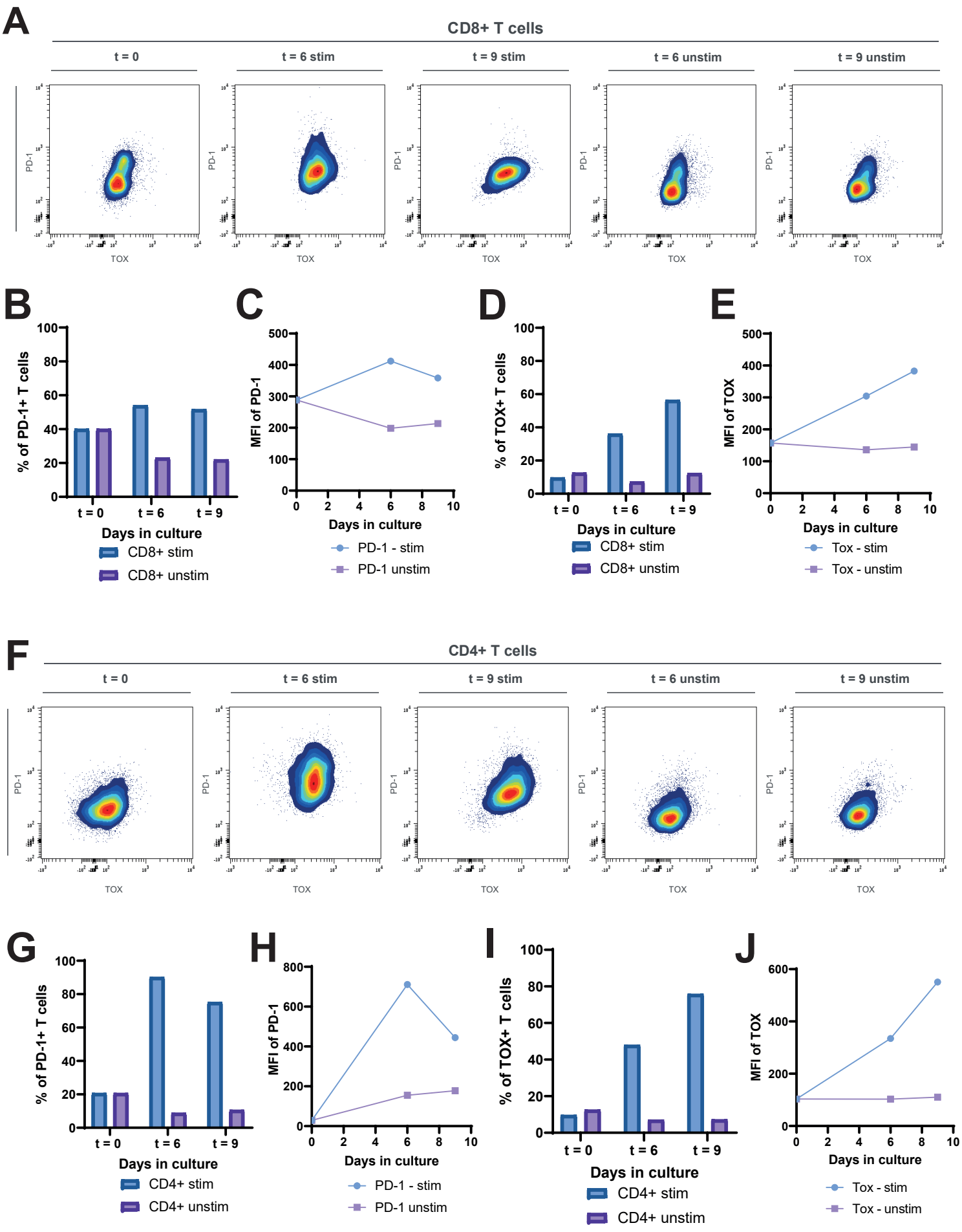

Fig. 5 Expression of hallmark T cell exhaustion proteins

A) Representative flow cytometric analysis of co-expression patterns of PD-1 and Tox expression in CD8+ T cells from culturing with CD3/CD28 beads. B) Fraction of PD-1+ in CD8+ T cell populations from culturing with CD3/CD28 beads. C) Median Fluorescent Intensity (MFI) of PD-1 in CD8+ T cells from culturing with CD3/CD28 beads. D) Fraction of TOX+ in CD8+ T cell populations from culturing with CD3/CD28 beads. E) MFI of TOX in CD8+ T cells from culturing with CD3/CD28 beads. F) Representative flow cytometric analysis of co-expression patterns of PD-1 and Tox expression in CD4+ T cells from culturing with CD3/CD28 beads. G) Fraction of PD-1+ in CD4+ T cells from culturing with CD3/CD28 beads. H) MFI of PD-1 in CD8+ T cells from culturing with CD3/CD28 beads. I) Fraction of TOX+ in CD4+ T cells from culturing with CD3/CD28 beads. J) MFI of TOX in CD4+ T cells from culturing with CD3/CD28 beads.

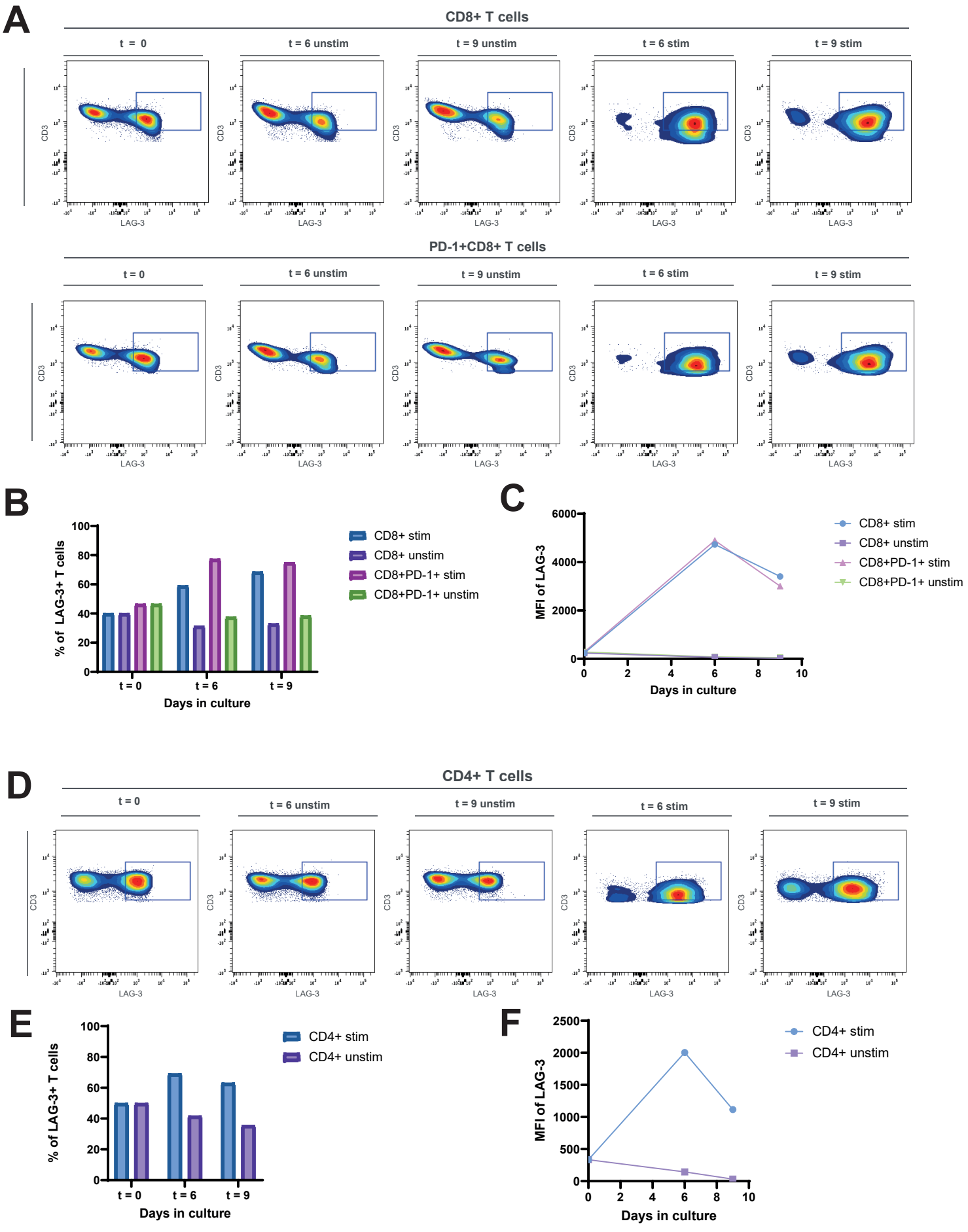

Fig. 6 T cell exhaustion hallmark – inhibitory immune checkpoint receptor expression
A) Representative flow cytometric analysis of expression patterns of LAG-3 in CD8+ and PD-1+CD8+ T cells from stimulating with CD3/CD28 beads. B) Fraction of LAG-3+ cells in CD8+and PD-1+CD8+ T cell populations from stimulating with CD3/CD28 beads. C) Median Fluorescent Intensity (MFI) of LAG-3 of CD8+ and PD-1+CD8+ T cell populations from stimulating with CD3/CD28 beads. D) Representative flow cytometric analysis of expression patterns of LAG-3 in CD4+ T cells from stimulating with CD3/CD28 beads. E) Fraction of LAG-3+ cells in CD4+ T cells froms stimulating with CD3/CD28 stimulating beads F) MFI of LAG-3 of CD4+ of T cells from stimulating with CD3/CD28 beads.
(Figure continues on next page)

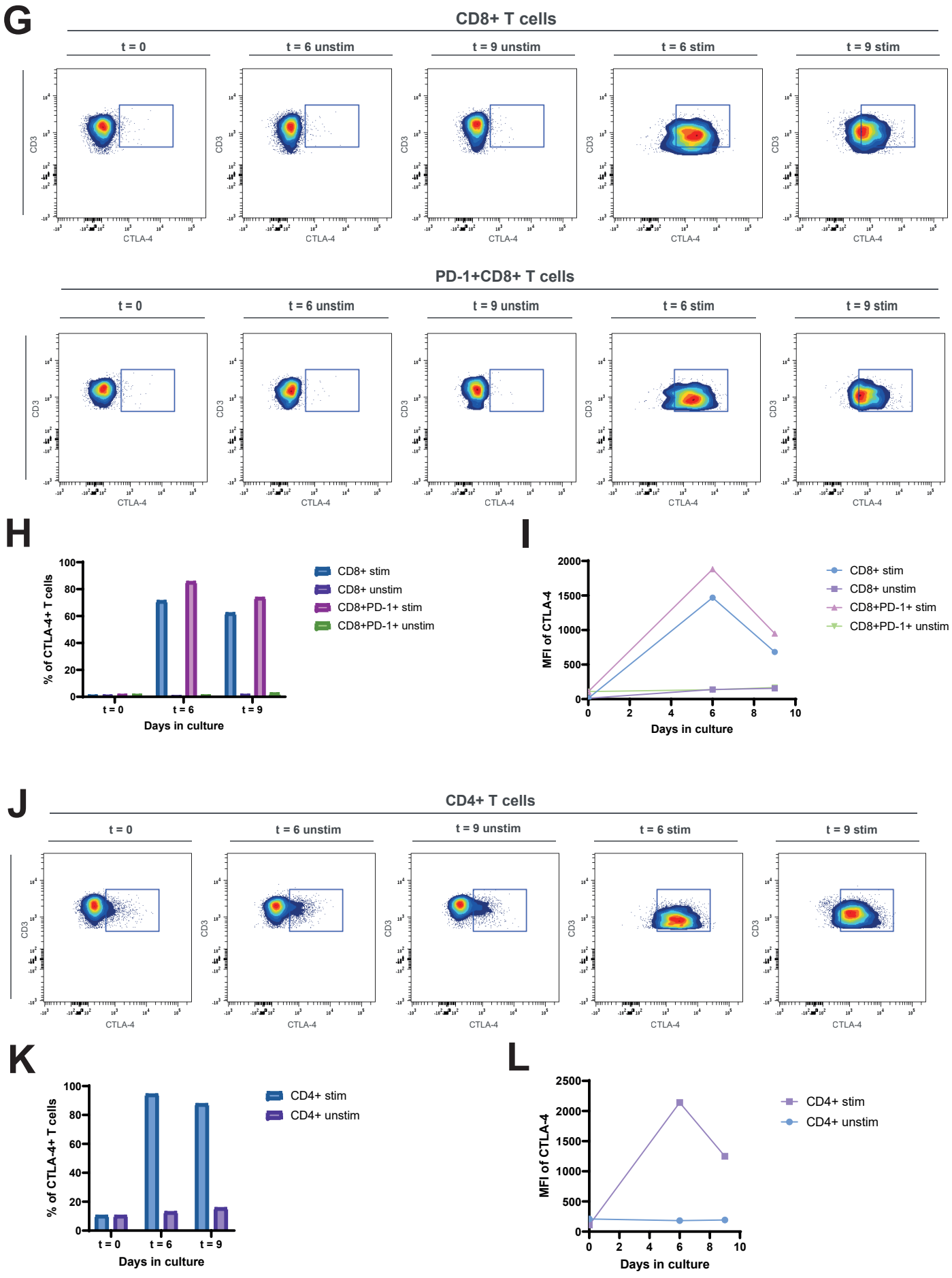

Fig. 6 T cell exhaustion hallmark – inhibitory immune checkpoint receptor expression (continued)
G) Representative flow cytometric analysis of expression patterns of CTLA-4 in CD8+ and CD8+PD-1+ T cells from stimulating with CD3/CD28 beads. H) Fraction of CTLA-4+ cells in CD8+and PD-1+CD8+ T cell populations from stimulating with CD3/CD28 beads. I) Median Fluorescent Intensity (MFI) of LAG-3 of CD8+ and PD-1+CD8+ T cell populations from stimulating with CD3/CD28 beads. J) Representative flow cytometric analysis of expression patterns of CTLA-4 in CD4+ T cells from stimulating with CD3/CD28 beads. K) Fraction of CTLA-4+ cells in CD4+ T cells froms stimulating with CD3/CD28 stimulating beads L) MFI of CTLA-4 of CD4+ of T cells from stimulating with CD3/CD28 beads.

CD8+ T cells stimulated by CD3/CD28 beads do not express Slamf6 and TCF-1 in a surrogacy relationship

TCF-1, a transcription factor relating to proliferative capacity of exhausted T cells, was interrogated for its relationship to the surface marker Slamf6, as it can be used as surrogate marker for TCF-1 levels in a murine system. In this instance, Slamf6 may allow for cell sorting of live cells demarcated by TCF-1 expression. In our human *in vitro* model, minor differences in Slamf6 expression were found (**Figure 7A, 7C and 7E**). Stimulated CD8+ and PD-1+CD8+ T cells displayed no changes in TCF-1 expression, whereas keeping them unstimulated in culture it increased. Even more so for unstimulated PD-1+CD8+, than global CD8+ T cells (**Figure 7B and 7D**). This could also be seen in the amount of TCF-1+ cells (**Figure 7D**). Regarding Slamf6 expression, this increased initially in unstimulated cultured cells and then returned to baseline of day 0. For the stimulated condition, this increased slightly and then dropped below baseline at day 9 (**Figure 7C**). These trends were observed in similar fashion regarding the fraction of cells that were Slamf6+ (**Figure 7E**), concluding that TCF-1 and Slamf6 are not expressed in a surrogacy relationship within this model.

CD8+ T cells stimulated by CD3/CD28 beads express CD69 after multiple days

CD69 is a marker of recent (4-6h) T cell activation that may have implications in immunophenotyping substages of exhaustion in PD-1+CD8+ T cells, with a loss of expression after activation and a return in Tex^{term}. Upon stimulation by CD3/CD28 beads for multiple days, CD69 is expressed a minority of cells (**Figure 8A**). Quantified, changes in MFI are minor (**Figure 8B**). However, a part of the T cells can be considered CD69+ in the stimulated condition, increasing over time which is not seen in the unstimulated T cells (**Figure 8C**).

CD8+ T cells stimulated by CD3/CD28 beads revoke Eomes expression, with the largest decrease in the PD-1+ cells

Eomes is a transcriptional regulator implicated play a role in initial stages of subset differentiation of exhausted T cells and interfere with bifurcation to a progenitor state of effector memory T cells (Tmem) (16,63). In mice, it is not expressed in naïve CD8+ T cells (64). For humans, this is not known. In mice it has been shown that in exhaustion through Eomes may be dynamically regulated with a decrease over intermediate subsets, e.g. Tex Tex^{prog2} and Tex^{int}, but returns in the terminally exhausted state, Tex^{term} (16). In this culture system, unstimulated CD8+ T cells show a Eomes+ and Eomes- population, shifting more towards Eomes- over time. In the unstimulated condition, these Eomes+ cells are found mostly within the PD-1+ cells of the CD8+ population (**Figure 9A**). Stimulation with CD3/CD28 beads decreased Eomes expression over time (**Figure 9B**), reducing the amount of Eomes+ cells in total after 6 days (**Figure 9B**). This was also observed in the fractions of Eomes+ cells between PD-1+CD8+ and CD8+ populations (**Figure 9C**). No distinct difference in overall expression or fraction of Eomes+ cells was found depending on if cells were PD-1+. These findings from Eomes expression in CD8+ T cells indicate that we induced an earlier developmental subset of T cell exhaustion, respectively Tex^{prog2} , but not Tex^{int} as observed through maintained TCF-1 expression (**Figure 7**)**.**

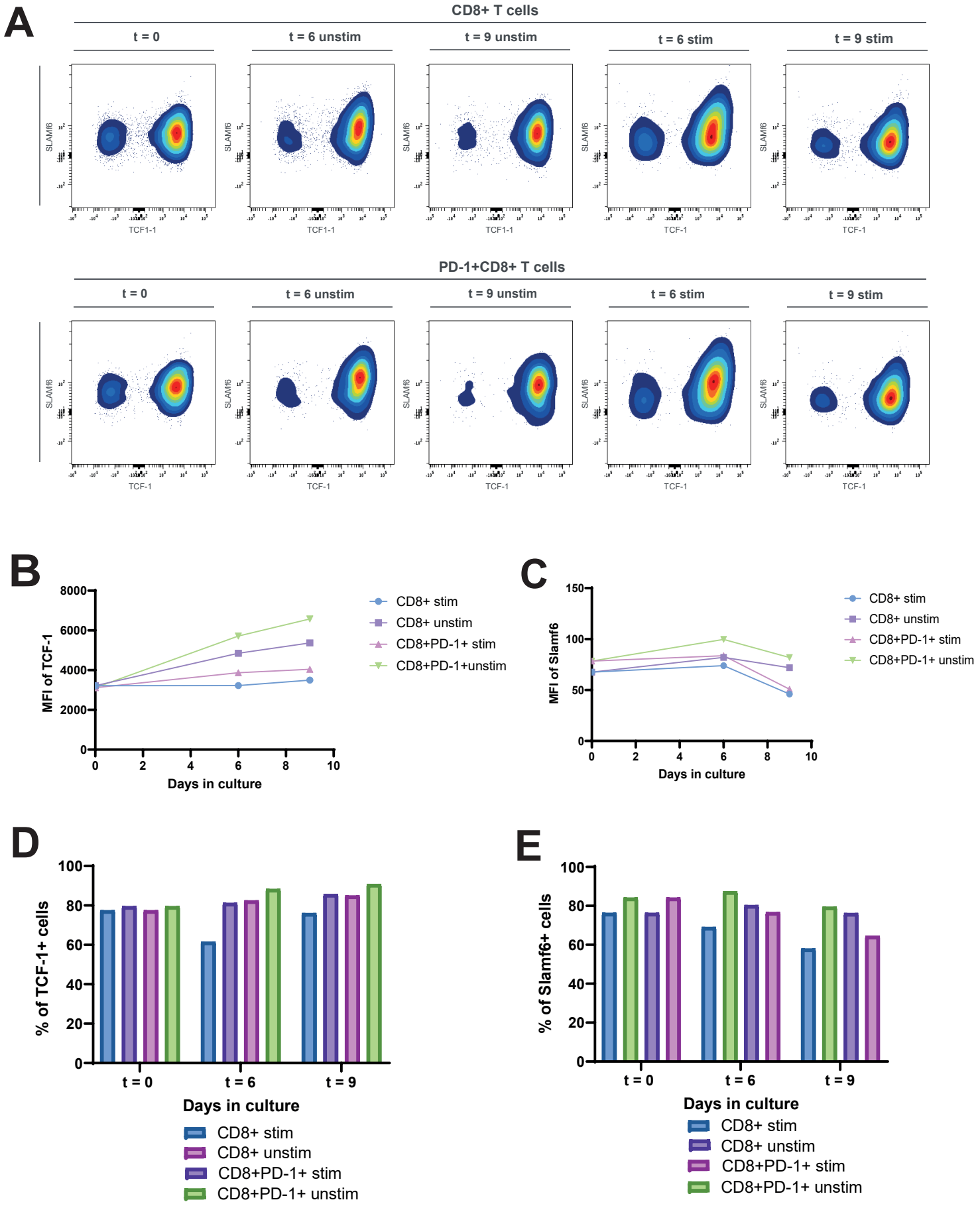

Fig. 7 Interrogation of Slamf6 as surrogate marker for TCF-1 in a human T cell exhaustion model
A) Representative flow cytometric analysis of expression patterns of Slamf6 and TCF1-1 in CD8+ and PD-1+CD8+ T cells from stimulating with CD3/CD28 beads. B) Median Fluorescent Intensity (MFI) of TCF-1 in CD8+ and PD-1+CD8+ T cell populations from stimulating with CD3/CD28 beads. C) MFI of Slamf6 in CD8+ and CD8+PD-1+ T cell populations from stimulating with CD3/CD28 beads. D) Fraction of TCF-1+ cells in CD8+ and PD-1+CD8+ T cell populations from stimulating with CD3/CD28 beads. E) Fraction of Slamf6+ cells in CD8+ and PD-1+CD8+ T cell populations from stimulating with CD3/CD28 beads.

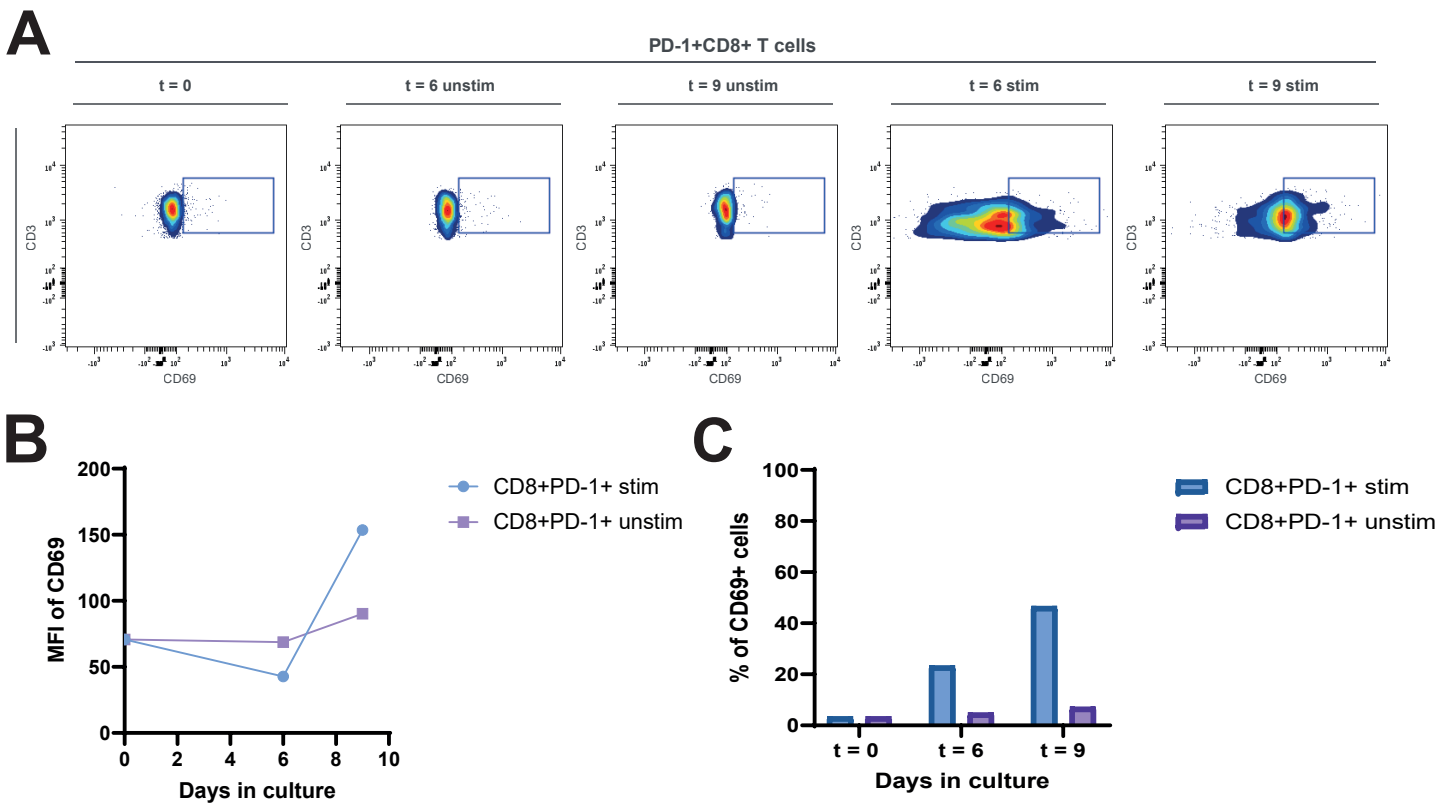

Fig. 8 Assessment of CD69 expression in a human T cell exhaustion model
A) Representative flow cytometric analysis of expression patterns of CD69 in CD8+PD-1+ T cells from stimulating with CD3/CD28 beads. B) Median Fluorescent Intensity (MFI) of CD69 in PD-1+CD8+ T cells from stimulating with CD3/CD28 beads. C) Fraction of CD69+ in PD-1+CD8+ T cells from stimulating with CD3/CD28 beads.

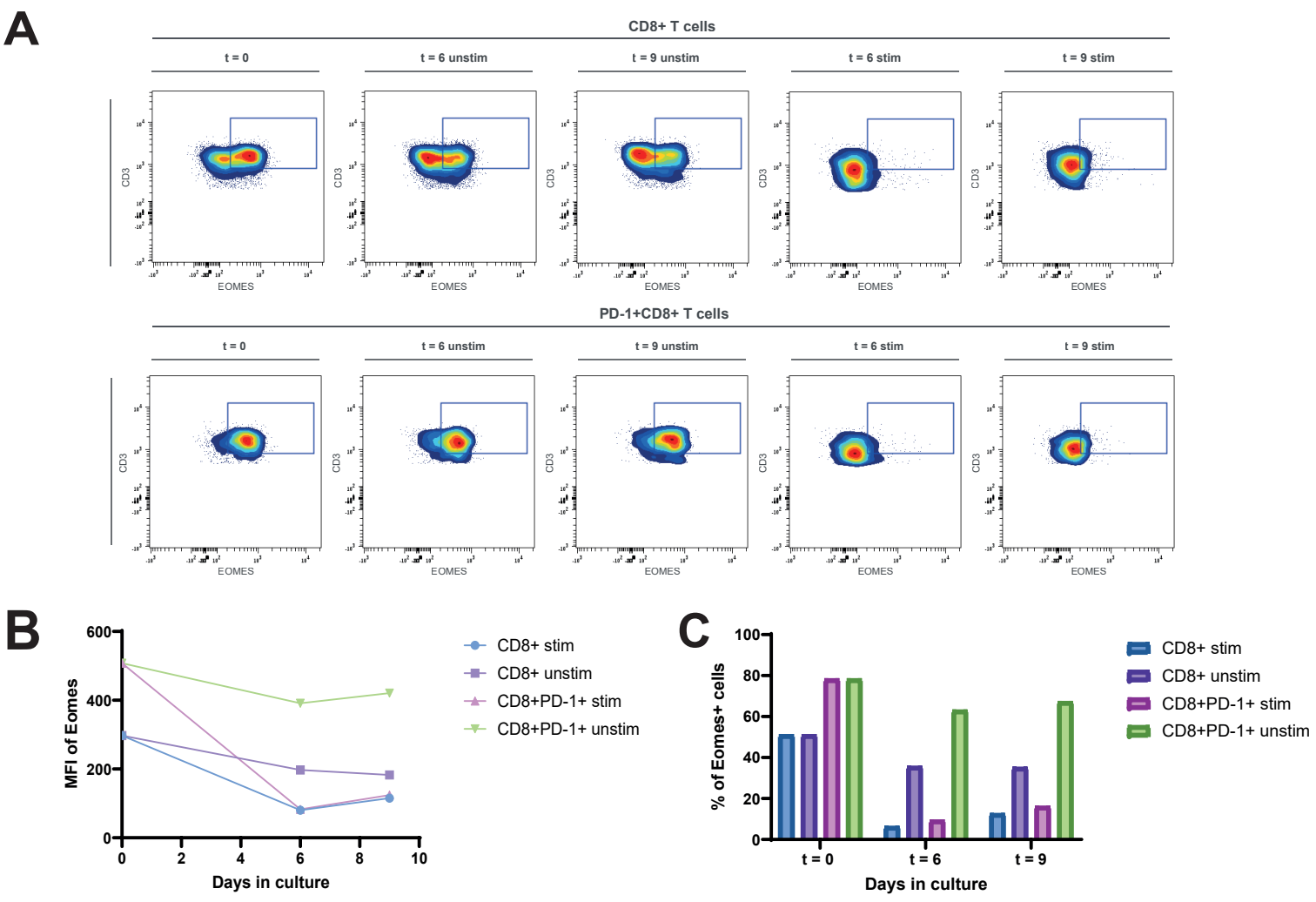

Fig. 9 Assessment of Eomes expression in a human T cell exhaustion model
A) Representative flow cytometric analysis of expression patterns of Eomes in CD8+ and PD-1+CD8+ T cells from stimulating with CD3/CD28 beads. B) Median Fluorescent Intensity (MFI) of Eomes in CD8+ and PD-1+CD8+ T cells from stimulating with CD3/CD28 beads. C) Fraction of Eomes+ in CD8+ and PD-1+CD8+ T cells from stimulating with CD3/CD28 beads.

DISCUSSION

In this study, we used T cells isolated from healthy donors to develop an *in vitro* model that mimics T cell exhaustion. T cell exhaustion was assessed using a 12-color flow cytometry panel that was designed and validated in this study. Applying the flow cytometry panel to the T cell culture system, which is based on chronic TCR and co-stimulation, we found hallmarks of T cell exhaustion, such as the expression of transcription factor TOX and inhibitory receptor PD-1, and the expression of multiple inhibitory receptors. Classically, studying T cell exhaustion relies on human tumor samples or murine tumor models. Studying the relationship between the TME, T cell exhaustion, and the (lack of) reinvigoration by ICPI can be simplified by employing an *in vitro* T cell exhaustion model for co-cultures or cytotoxicity assays.

Optimization of cell culture for model generation

We used and optimized an existing protocol to further study its potential to model T cell exhaustion (65). We chose to culture the cells for 72h before washing and refreshing medium as the medium indicated this was a suitable timeframe. In contrast to the protocol from Dunsford et al., we decided to retain the same pool of CD3/CD28 beads added on day 0, as the removal of the beads leads to cell loss of the bead-bound fraction that contains TCR-stimulated cells, skewing results towards a free fraction that has received decreased stimulation. We adhered to the recommended bead-to-cell ratio of 1:1 by adding beads upon increasing the cell counts in the culture.

To assess cell viability, we noted cell counts and stained cells for viability in the flow cytometry experiments. Under unstimulated conditions, cell shrinkage and cell death were observed. This indicates the need for IL-2 concentration optimization in culture, as well as attentiveness to cell culture contamination. Under stimulated conditions, the cells proliferated and expanded. Depending on the cellular concentration, the cells intended for staining were either washed and resuspended in less medium or directly plated for staining. This may have affected the amount of cellular debris and dead cells in the samples. This led to unreliable viability measurements based solely on the LIVE/DEAD nIR 780 viability stain (**S6A and S6B**). However, the stain was still included in the flow cytometry panel to optimize the analysis of the measured cells, allowing for the exclusion of dead cells for more reliable results. By measuring absolute live cell numbers, we observed diminishing cell numbers in the unstimulated condition compared to the stimulated condition (**S6C**). The unstimulated condition contains naïve T cells which proliferate very little, whereas T cell activation occurs upon stimulation of the T cell receptor by CD3/CD28 beads, leading to an increase of proliferation. As these absolute cell counts are based on live cells, it cannot be ascertained how the balance lies between proliferation and cell death. To use this model, cell viability of unstimulated cells must be increased to rule out confounding results imposed by cellular stress from its culturing conditions.

Decisions in gating strategy

Firstly, we cleaned up signal by gating out debris, double events, and dead cells (**Figure 4A, 4B and 4C**). CD3 comes in multiple isoforms and is part of the TCR (66). CD8 serves as a co-receptor for the TCR and plays a role in the interaction of T cells and their respective antigen. It is specific to MHC I, found on antigen presenting cells (67). Next, we gated for cytotoxic T cells based on pan-T cell marker CD3 and CD8 for the cytotoxic lineage (**Figure 4D**). As MACS separation does not have 100% purity in yield, some CD3- was expected. When gating for CD3+CD8+, a comparison was made between unstained samples, freshly isolated T cells stained with the full panel, and a PBMC sample with a single CD8 stain to determine the CD8 threshold coordinates.

Following this, we gated PD-1+ cells. The PD-1 threshold x-axis coordinates of the gate were determined based on the PBMC PD-1 single staining. The sample was not stained for CD3; as such, it was not suitable for determining the y-axis coordinates. For this purpose, a fully stained sample from t = 0 d was used (**Figure 4E**). Sustained upregulation of PD-1 is a hallmark of T cell exhaustion and is therefore important for gating (68). We also gated for TOX, an important transcription factor for T cell exhaustion (12) (**Figure 4F**). Following the PD-1 gate, we gated separately for remaining markers. Determining the threshold on the x-axis was determined by comparing an unstained sample to a single stain and for the y-axis, an unstained sample, and a full panel stain on T cells (**Figure 4G**). After gating for viable cells, we set another gate for CD4+ T cells based on CD4 and CD3, as CD4 T cells may influence a co-culture and can show some aspects of exhaustion (44). In further analysis CD3+PD-1+CD8+ cells are compared further to the CD3+CD8+ and CD3+CD4+ population PD-1- cells expressing other relevant markers can influence the system as a whole and its use in further assays.

For a negative control we stained cells and checked expression after gating for debris and single events (**Figure 4A and 4G).** They did not express targets found within our panel, except for TCF-1. TCF proteins are key players in the Wnt-pathway (69). According to previous reports, TCF-1 is expressed predominantly in T cells, but can be found in many other tissues. Unsurprisingly, HEK293T cells showed positive staining for TCF-1, as it is expressed in low amounts in many tissues (**S5**). Due to time constraints, we were unable to acquire a TCF-1- expressing line or TCF-1 KO line. Finally, we regret not including a PBMC (stimulated) control sample stained for the full panel to set gates more accurately on the x- and y-axes combined.

PD-1 and TOX expression in CD8+ T cells

T cell exhaustion has been described in chronic viral infection in murine models by at least sustained upregulation of PD-1, among other inhibitory receptors (70,71), and similar processes have been found in human infection and tumor infiltrating CD8+ T cells (18,72). We found that in our culture system over time T cells upregulated PD-1 leading to more cells being both PD-1+ and an increase in MFI (**Figure 5**). This is in line with the reports that this is a result of sustained TCR signaling, which we achieve by continuously stimulating the receptor with CD3/CD28 beads (70). CD8+ T cells that were PD-1- may represent a fraction that has not been activated by the beads. As gating excludes double events, bead-bound cells may be excluded from analysis. To note, PD-1 expression is not a decree of T cell exhaustion, as it has also been found that T cells can differentiate into and exhausted-like stage expressing other inhibitory receptors without the expression of PD-1 (73). Clearly defined populations with differing PD-1 levels could not be found in our *in vitro* model, although the intensity of expression may be highly relevant to functionality. It has been shown that PD-1+CD8+ T cells with intermediate expression compared to high, responded better to blockade of the PD-1/PD-L1 axis (74). PD-1+ intermediate subsets, together with TCF-1- delineated Tex^{int} from Tex^{term} in the model of Beltra et al., In our *in vitro* model, we did not find a third PD-1^{hi} expressing population. This fits with our findings of TCF-1 expression, discussed later, indicating our cells are in the Tex^{prog2} stage

TOX is a transcription factor that epigenetically programs T cells to commit to an exhausted fate. It is critical for T cells to develop into an exhausted state whereas not necessary for effector and memory T cells and repressing epigenetic events specific to forming effector T cells (12). In our results we find increased expression of TOX under stimulation with CD3/CD28 beads, indicating that TOX can be induced by TCR stimulation. Driving T cell exhaustion fate through TOX can possibly be achieved in this manner but is not limited to TCR stimulation as it can be induced with solely cytokines IL-12/-15/-18 (75). TOX is an established but not exclusive marker for T cell exhaustion: its prolonged expression indicates exhaustion; however, this prolonged expression has been described for durations of 10 up to 30 days (12). Here, the model expression has only been measured for up to nine days at 3-day intervals. We believe that inducing TOX expression can indeed induce exhaustion; however, we did not investigate whether this can be sustained for a longer time *in vitro*. Further confirmation of the driving transcriptional effects of TOX should be performed using single-cell RNA sequencing (scRNA-seq), considering that T cells within the culture may be in different exhaustion states. Previous reports on the effects of TOX involve T cells subjected to infection or tumor presence for weeks to months (12,16).

Identifying the stage of exhaustion is important because the point of terminal exhaustion comes with no longer possible reversion, which is relevant to the efficacy of response to ICPI (76,77). There have been reports of epigenetic ‘scarring’ which are irreversible changes in exhausted T cells that do not reverse when eliminating the persisting antigen (13,14). This lack of epigenetic plasticity is largely attributed to reprogramming via TOX (13). The clonal replacement of a subset of exhausted T cells fits the model that cells past this point of no return, for example, Tex^{term}, does not show a durable response to ICPI (77). Chronic TCR signaling is necessary but also sufficient alone to induce exhaustion *in vitro*, and these epigenetic scars rely primarily on TCR signaling and less an inflammatory environment (14,78). Since T cells can acquire restored effector function when removed from context, these cells could remain only ‘scratched’ (79). Investigating the changed chromatin states after several time points of bead stimulation should use single-cell ATAC-seq. The amount of given TCR signals before the ‘scars’ appear, remains elusive and if we can immunophenotypically monitor this from human samples.

Inhibitory receptors expressed by stimulated T cells in culture.

One characteristic of T cell exhaustion is the expression of multiple inhibitory receptors, such as CTLA-4, TIM-3, LAG-3, and TIGIT, with ligands found on antigen-presenting and tumor cells in the TME, thereby decreasing effector function (72). The inhibition of checkpoint activity by blocking receptors with monoclonal antibodies has been exploited therapeutically. CTLA-4, which competes for binding to CD80/86, inhibits T cell function by interfering with signaling through CD28 (80,81). Blocking this immune checkpoint with ipilimumab combined with PD-1 blocking with nivolumab has shown improved results compared to blocking with single agents alone in advanced melanoma (59). In our study, we found elevated expression of the immune checkpoints PD-1, CTLA-4, and LAG-3 in CD8+ T cells (**Figure 5A, 6A and 6G**). Upregulation of immune checkpoints is associated with decreased TCR and co-stimulatory signaling (82). PD-1 expression is not a prerequisite for the expression of other inhibitory receptors, which concurs with previous reports (73). There have been reports showing that both the expression levels and repertoire of inhibitory receptors increase with progressive exhaustion of CD8+ T cells (16,54). This panel contains three established inhibitory receptors, with arguably a fourth being Slamf6 (49,83). Regarding the model from Beltra et al., half, or more cells in Tex^{prog1} Tex^{prog2} expressed 1-3 different inhibitory receptors. In further exhaustion stages Tex^{int} and Tex^{term}, the cells showed co-expression of 3-4 inhibitory receptor in more than half of all cells (16). Further studies of this model could include measuring more alternative immune checkpoints to demonstrate increased expression and complexity in co-expression of inhibitory receptor profile. Regarding these profiles, it is likely context dependent as inhibitory receptor profiles differ between virus responsive and tumor reactive T cells. To add, inhibitory receptor profile has been linked to anatomical location and differentiation stage (84). We believe that the expression of CTLA-4 and the LAG-3 inhibitory receptor on CD8+ T cells in this model demonstrates T cell exhaustion. However, we did not include further inhibitory receptors in our panel so can conclude this to some extent

TCF-1 expression cannot be substituted by Slamf6 in CD8+ T cells in a human in vitro culture system for T cell exhaustion

TCF-1 is a T cell-specific transcription factor that plays a role in self-renewal of murine embryonic stem cells and commits lymphoid progenitors in the bone marrow to the innate lymphoid cell lineage (85). T cell development in primary lymphoid tissues and differentiation to mature T cells in the periphery require TCF-1 (86). More recently, TCF-1 has been suggested to regulate the function and maintenance of CD8+ exhausted T cells (45,46,87). The role of TCF-1 has been shown to be indicative of a four-stage developmental differentiation process with a gradual decrease of TCF-1 expression (**Figure 1**). In line with previous reports, precursor exhausted T cells replenish the pool of exhausted T cells and their expansion upon PD-1 blockade, revealing earlier more potent subsets that could predict response to immunotherapy (74,88). Previously, Slamf6 has been found to be applicable as a surrogate marker for TCF-1 and indicates earlier stages of exhaustion in mice, respectively, Tex^{prog1} and Tex^{prog2} (16,45). As a surface marker could enable subset identification and sorting of live cells, we interrogated the relationship between Slamf6 and TCF-1 to assess if this can also be linear in a human *in vitro* model.

In our study, we found that the MFI of TCF-1 increased by maintaining the cells in culture without stimulation (Figure 6B). Regarding the fraction of TCF-1+ cells, we found that upon stimulation with CD3/CD28 beads, the fraction of TCF-1+ cells slightly decreased within 6 days for the CD8+ population (**Figure 7D**). Slamf6 expression showed minor changes in both the positive fraction and the MFI (**Figure 7C and 7E).** We could not observe a clear expression relationship; thus, this surrogacy connection was not reproducible in this human *in vitro* culture system. As TCF-1 expression did not shift to a TCF-1- population, this is indicative of early T cell exhaustion (Tex^{prog1} and Tex^{prog2}), and the T cells in this *in vitro* system were not pushed to further exhaustion stages, Tex^{int} and Tex^{term}, respectively.

Slamf6 expression has been reported to increase by > 2-fold in human cells upon stimulation with α-CD3 for up to 6 days (83). Our first measured time point was at t = 6 days, which shows an increase, but this was < 2-fold. Focusing on TCF-1 on its own could show a link to T cell exhaustion. We report no decrease, but consistent expression upon stimulation. TCF-1 in mature CD8+ T cells regulates early divergence between the terminal effector and precursors of T cell exhaustion, and plays a role in maintaining the stem-cell-like pool of exhausted T cells in mice (45). Very recent work has shown that CD8+TCF-1+ in persistent infection can have vastly different epigenetic states, either diverging to either memory T cells or exhausted T cells; thus, TCF-1 expression in activated CD8+ T cells cannot solely define the stem cell biology of exhausted T cells (89). Nonetheless, CD8+TCF-1+ can give rise to TCF-1- CD8+ T cells after

adoptive transfer in 21 days of chronic LCMV infection (16). This demonstrates the need for our system to examine the effects of longer timeframes to rule out the possibility that TCF-1- cells cannot be generated in this *in vitro* culture system. It is highly relevant to further induce exhaustion in the *in vitro* model to control for exhaustion stage and investigate relationship to ICPI response. TCF-1+PD-1+ T cells show improved response to ICPI (39,74,90). To completely rule out that it is not possible to use Slamf6 as a surrogate marker in a human *in vitro* T cell exhaustion system, it should be able to show a loss of TCF-1 expression with cells that concurrently lose Slamf6. Demonstrating multiple stages of exhaustion, up until Tex^{term}, is essential to use the *in vitro* model for assessment of other TME players and their involvement in both exhaustion stage as well as ICPI response.

CD69, a marker for recent activation and exhaustion stage

In the *in vivo* model described by Beltra et al., Slamf6 (as a surrogate marker for TCF-1) and CD69 mark developmental substages of exhausted T cells. This could distinguish PD-1 ^{int}TCF-1- from PD-1^{hi} TCF-1-. The use of CD69, together with Slamf6, could therefore delineate substages with surface markers in a qualitative fashion, meaning that quantitative PD-1 control with multiple expression levels is not necessary (16). Following the *in vivo* model of Beltra et al., Tex^{prog1} shows CD69 expression, which disappears in Tex^{prog2} and Tex^{int} following a return to Tex^{term} (**Figure 1**).

We observed some expression of CD69 upon stimulation, although this was <50% in all cells (**Figure 8C**). This could represent a fraction of T cells that were recently activated in culture by previously not making contact with the bead. Additionally, it has been reported that CD69 expression increases upon T cell activation but subsides after 4-6 hours (91). In line with this, CD69 showed an increase in the bead-bound fraction at earlier time points. Our first measured time point was after 6 days. Including a recent activation condition (e.g., 1-2 h) can be used as a control. In contrast, T cells expand rapidly several hours after activation (17). As this would increase the proportion of activated T cells to inactivated cells in the culture, this would not be in line with the argument when CD69+ T cells increased between days 6 and 9 (**Figure 8B and 8C**). A return of CD69 expression may indicate a terminally exhausted T cell, although more characteristics must be confirmed, which will be discussed later (16). To determine whether CD69 expression is more recent or has returned to previously activated cells, this should be confirmed in future experiments that assess the expression of the free and bead-bound fractions separately. This could be used to monitor the activation speed and efficiency of CD3/CD28 beads. For instance, using an established triple reporter activation cell line could visualize and quantify the likelihood of certain time points to show CD69 expression due to recent activation or later return (92). Selecting a timepoint in which only bead-bound cells cultured further may optimize the *in vitro* system.

Taking the proposed model of Beltra et al., we see in our results that our cultured cells might follow this pattern with cells being in the Tex^{prog2} and Tex^{int} stages, given that TCF-1 should decrease over time in culture (**Figure 7D**). As the cells are mostly TCF-1+, they are more likely to represent Tex^{prog2}. Retaining this model, one can hypothesize that further culturing in the presence of beads, thus prolonging TCR stimulation, will lead to progression to further stages. However, in Beltra et al.'s model, the most terminally exhausted state shows a return in CD69 expression, which is also an established marker of tissue residency in rebounded expression (93). In the work of Beltra et al., the melanoma *in vivo* model showed Tex^{term} accumulation in tissue, which raises the question of whether CD69 expression as a terminal exhaustion marker lies within the characteristics of being tissue resident and not exhaustion per se. Although these findings suggest a positive association between terminal exhaustion and CD69 expression, further understanding of the directional effects requires thorough and careful examination, as it may be possible that the return of expression of this marker, as in Tex^{term}, will not be achieved *in vitro.* Our model could use CD69 in immunophenotyping, but it is necessary to evaluate whether it occurs due to recent activation or whether it is a later return of expression.

The return of Eomes expression may require more time

The transcriptional regulator Eomes plays a crucial role in the formation and function of effector and memory CD8+ T cells (94). It is also implicated in progenitor subsets of exhausted T cells (47,95). Here, we show that Eomes expression revoked in our *in vitro* culture system, leaving unstimulated cultured T cells to partially retain Eomes (**Figure 9**). Eomes expression is downstream of TCF-1 (45). In our model, TCF-1 did not clearly decrease upon bead stimulation (**Figure 7**), which concurs with our observation of decreased Eomes expression. Following the developmental framework of Beltra et al., low Eomes expression was observed in Tex^{prog2} and Tex^{int}, which does not match our findings regarding CD69 and TCF-1 (**Figure 7 and 8**).

Notably, Eomes is linked to the transcription factor T-bet, which controls PD-1 expression (96). Nuclear Eomes:T-bet ratio is relevant, as both compete for DNA binding, and this ratio is elevated in exhausted T cells compared to that in memory T cells. This nuclear transcription factor ratio changes upon PD-1 blockage in mice and is associated with a lower Eomes:T-bet ratio (96). Including T-bet staining to Eomes and using Imagestream analysis may allow for more thorough inquiry of Eomes implications in T cell exhaustion and perhaps an additional readout for PD-1 blockage response next to cytotoxicity assays.

Interestingly, Eomes and CD69 in effector memory T cells (CD45RO+) are associated with response to ICPI in melanoma patients (97,98). Differentiation to progenitor effector memory T cells is under control of transcription factor Hobit, which is antagonized by Eomes (63). In Beltra et al., most Tex^{term} have rebounded Eomes and CD69 expression and are tissue-bound. Further studies could investigate the role of Hobit for T cells to branch to effector memory; if rebounded Eomes expression can be linked to a lack of ICPI response due to insufficient differentiation to effector memory resident T cells.

T cell exhaustion characteristics in CD4+ T cells

In describing T cell exhaustion, CD8+ T cells are mostly of focus. However, debate exists whether CD4+ T cell exhaustion exists. They can express inhibitory receptors decreased cytokine production (44). However, it is not understood yet if they show similar changes in metabolism and epigenetic profile as CD8+ T cells do. As CD4+ T cells were also present in our culture system based on pan-T cells, this affects their use in further co-cultures.

We observed increased PD-1 and TOX expression in CD4+ T cells, which are hallmarks of exhaustion (**Figure 5F**). Additionally, we observed expression of multiple inhibitory receptors in CD4+ T cells, including PD-1, LAG-3 and CTLA-4 (**Figure 5F, 6D and 6J**). We observed LAG-3 expression on CD4+ T cells. It is an inhibitory receptor that competes with CD4 to bind to MHC II, thereby impeding CD4+ T cell activation (99). In this culture system, CD4+ T cells do not require MHC II for activation and are instead activated by beads. We found LAG-3 expression in CD4+ and CD8+ populations, which was already present before activation and increased when stimulated with beads. The highest expression was observed in the CD8+ cell population (**Figure 6E and 6F**).

CTLA-4 is constitutively expressed on CD4+ Tregs, which are also characterized by FOXP3 and CD25 expression. We observed higher levels of CTLA-4 expression in CD4+ compared to CD8+ populations (**Figure 6G and GJ)**. Tregs in cancer exert suppressive functions by competing with CD28 for CD80/CD86, thereby affecting CD8+ T cell co-stimulation (100). Intratumoral Tregs are preferentially depleted through ICPI targeting CTLA-4, as they express higher levels than other Tregs in the circulation and thymus (101). In our culture system, the presence of CTLA-4 did not lead to decreased CD8+ stimulation, as the natural ligand, CD80/CD86, was substituted by bead stimulation. However, when employing this culture system in co-culture with other cell types, competitive binding can occur that influences T cell signaling. Furthermore, differing levels of CD4+ T cells expressing the majority of CTLA-4 affect the outcomes of ICPI targeting this receptor. This underlines the importance of assessing CTLA-4 expression in culture system before testing additional factors in co-culture.

Future project perspectives

An important remark about our study is the absence of statistical analysis. After technical validation of the flow cytometry panel, we were able to obtain one single useful dataset of the culture system based around one donor. Inter-donor variability requires more measurements and accounts for measurement variability, with an internal control for normalization. Although preliminary results show promising aspects of the model, caution should be taken, and we urge further repetitions to demonstrate its reproducibility. This project investigated immunophenotypes and left room for functional characteristics to be addressed. Proliferation rates were not addressed, but could be assessed in the future with CSFE cell proliferation assays. We hypothesize that CFSE would be high on t = 0 days and decrease over time upon stimulation, indicating proliferation. For more prolonged stimulation, we expect CSFE signal to remain high after staining. We did not yet address T cell exhaustion characteristics such as proliferation. We did count absolute cell numbers from the culture; however this cannot be used as a readout for proliferation (**S6B**). Additionally, with T cell exhaustion decrease of cytokine production is observed (22). To address cytokine profiles, ELISA of culture supernatant would be of recommendation. As this is a bulk method for a population of T cells that may reside in various stages of

exhaustion, sorting methods with consecutive PCR can be employed. Learning about the cytokine profiles of these cells may bring insight into their cytotoxic capabilities and there is opportunity to investigate this further with co cultures. Lastly, the prominent lack of effector function could be demonstrated with a killing assay.

Conclusion

In this study, we aimed to establish a human *in vitro* culture system for T cell exhaustion by investigating its potential using an 11-marker flow cytometry panel. We technically validated the panel and ran it on T cells collected at different time points from the *in vitro* culture system, providing us with a dataset that shows some characteristics of (upcoming) T cell exhaustion. Through the expression of PD-1, TOX, multiple inhibitory receptors, TCF-1, and Eomes, we project that cells were transformed into Tex^{prog1} and Tex^{prog2} states.

Considering that our culturing method did not fully did not reach Tex^{term} stage, it is likely that the duration of the stimulation was too short. As *in vivo* exhaustion takes multiple weeks to develop, it is understandable that others' efforts to induce T cell exhaustion *in vitro* have cultured T cells for up to 35 to 49 days, longer than our current model (102,103). To speed up the process, there may be opportunities to induce T cell exhaustion through metabolic regimens, such as culturing in a hypoxic environment, supplementation of potassium, or decreasing glutamine in the medium, as these TME occurrences can restrict T cell function (104–106). However, this would only be suitable for establishing a terminally exhausted state before reverting culturing conditions to medium with IL-2, as retaining these culturing conditions would affect other cell types in co-culturing studies. As theorized by Yost et al., a stem cell pool of T cells may expand upon PD-1 blockade as observed by the clonal expansion of PD-1+TCF+ CD8+ T cells (77). Upon entering the TME, these T cells encounter several factor that push them to become terminally exhausted. A human *in vitro* culture system combined with the actors of this process, could therefore bring insight to lack of ICPI response.

Overall, a human *in vitro* exhaustion system would facilitate the exploration of specific tactics intended to delay or reverse T cell exhaustion using ICPI in a simple, affordable, and quick manner. However, more work is required to induce and characterize *in vitro* exhausted T cells and validate their development through several stages of exhaustion.

ACKNOWLEDGEMENTS

I would like to express my gratitude to Dr. Yvonne Vercoulen for facilitating my internship at her research group and in addition to this: the supervision near the end of my internship, her patient demeanor, and confidence in me. Additionally, I extend my thanks to Stephanie van Dam for familiarizing me with the lab and technical training of equipment. I would like to give our lab technicians thanks for the training I received in the lab and advice organizing experiments. A big thank you goes out to Thijs Demmers, my fellow student in the lab helping me start up. Collaborating, we shared lab time and organized similar techniques together for efficiency. Furthermore, I am thankful for the flow cytometry expertise and enthusiasm Rowena Melchers provided at the Flow Facility. I am also grateful to many technicians within the CMM for advice, training and feedback. I am grateful for the meaningful and scientific conversations I had with many people working in the CMM and the joys I experienced with fellow lab mates and in the office fellow interns. Lastly, I would like to acknowledge my study coordinator, Dr. Lisa Groenendaal–van Weert, for assisting in the organization of my study program and counselling in times of need.

REFERENCES

1. Alexandrov LB, Kim J, Haradhvala NJ, Huang MN, Tian Ng AW, Wu Y, et al. The repertoire of mutational signatures in human cancer. Nature 2020 578:7793 [Internet]. 2020 Feb 5 [cited 2022 Sep 23];578(7793):94–101. Available from: https://www.nature.com/articles/s41586-020-1943-3

2. Matsushita H, Vesely MD, Koboldt DC, Rickert CG, Uppaluri R, Magrini VJ, et al. Cancer exome analysis reveals a T-cell-dependent mechanism of cancer immunoediting. Nature [Internet]. 2012 Feb 8 [cited 2022 Sep 23];482(7385):400–4. Available from: https://www.ncbi.nlm.nih.gov/pmc/articles/pmid/22318521/?tool=EBI

3. Fridman WH, Zitvogel L, Sautès-Fridman C, Kroemer G. The immune contexture in cancer prognosis and treatment. Nature Reviews Clinical Oncology 2017 14:12 [Internet]. 2017 Jul 25 [cited 2022 Nov 17];14(12):717–34. Available from: https://www.nature.com/articles/nrclinonc.2017.101

4. Paijens ST, Vledder A, de Bruyn M, Nijman HW. Tumor-infiltrating lymphocytes in the immunotherapy era. Cellular & Molecular Immunology 2020 18:4 [Internet]. 2020 Nov 2 [cited 2022 Sep 23];18(4):842–59. Available from: https://www.nature.com/articles/s41423-020-00565-9

5. Cheng H, Ma K, Zhang L, Li G. The tumor microenvironment shapes the molecular characteristics of exhausted CD8+ T cells. Cancer Lett. 2021 May 28;506:55–66.

6. Wang Y, Hu J, Li Y, Xiao M, Wang H, Tian Q, et al. The transcription factor Tcf1 preserves the effector function of exhausted CD8 T cells during chronic viral infection. Front Immunol. 2019;10(FEB):169.

7. Sandu I, Cerletti D, Oetiker N, Borsa M, Wagen F, Spadafora I, et al. Landscape of Exhausted Virus-Specific CD8 T Cells in Chronic LCMV Infection. Cell Rep. 2020 Aug 25;32(8):108078.

8. McLane LM, Abdel-Hakeem MS, Wherry EJ. CD8 T Cell Exhaustion During Chronic Viral Infection and Cancer. https://doi.org/101146/annurev-immunol-041015-055318 [Internet]. 2015 Apr 16 [cited 2022 Sep 23];37:457–95. Available from: https://www.annualreviews.org/doi/abs/10.1146/annurev-immunol-041015-055318

9. Li H, van der Leun AM, Yofe I, Lubling Y, Gelbard-Solodkin D, van Akkooi ACJ, et al. Dysfunctional CD8 T Cells Form a Proliferative, Dynamically Regulated Compartment within Human Melanoma. Cell. 2019 Feb 7;176(4):775-789.e18.

10. Sekine T, Perez-Potti A, Nguyen S, Gorin JB, Wu VH, Gostick E, et al. TOX is expressed by exhausted and polyfunctional human effector memory CD8+ T cells. Sci Immunol [Internet]. 2020 Jul 1 [cited 2022 Nov 18];5(49). Available from: https://www.science.org/doi/10.1126/sciimmunol.aba7918

11. Goding SR, Wilson KA, Xie Y, Harris KM, Baxi A, Akpinarli A, et al. Restoring immune function of tumor-specific CD4+ T cells during recurrence of melanoma. J Immunol [Internet]. 2013 May 5 [cited 2022 Nov 18];190(9):4899. Available from: /pmc/articles/PMC3633733/

12. Khan O, Giles JR, McDonald S, Manne S, Ngiow SF, Patel KP, et al. TOX transcriptionally and epigenetically programs CD8+ T cell exhaustion. Nature 2019 571:7764 [Internet]. 2019 Jun 17 [cited 2022 Oct 8];571(7764):211–8. Available from: https://www-nature-com.proxy.library.uu.nl/articles/s41586-019-1325-x

13. Abdel-Hakeem MS, Manne S, Beltra JC, Stelekati E, Chen Z, Nzingha K, et al. Epigenetic scarring of exhausted T cells hinders memory differentiation upon eliminating chronic antigenic stimulation. Nature Immunology 2021 22:8 [Internet]. 2021 Jul 26 [cited 2022 Nov 3];22(8):1008–19. Available from: https://www.nature.com/articles/s41590-021-00975-5

14. Yates KB, Tonnerre P, Martin GE, Gerdemann U, al Abosy R, Comstock DE, et al. Epigenetic scars of CD8+ T cell exhaustion persist after cure of chronic infection in humans. Nature Immunology 2021 22:8 [Internet]. 2021 Jul 26 [cited 2022 Nov 4];22(8):1020–9. Available from: https://www.nature.com/articles/s41590-021-00979-1

15. ElTanbouly MA, Noelle RJ. Rethinking peripheral T cell tolerance: checkpoints across a T cell's journey. Nature Reviews Immunology 2020 21:4 [Internet]. 2020 Oct 19 [cited 2022 Nov 7];21(4):257–67. Available from: https://www.nature.com/articles/s41577-020-00454-2

16. Beltra JC, Manne S, S. Abdel-Hakeem M, Schuchter LM, Huang AC, Wherry JE. Developmental Relationships of Four Exhausted CD8+ T Cell Subsets Reveals Underlying Transcriptional and Epigenetic Landscape Control Mechanisms. Immunity. 2020;52:1–17.

17. Kaech SM, Wherry EJ, Ahmed R. Effector and memory T-cell differentiation: implications for vaccine development. Nature Reviews Immunology 2002 2:4 [Internet]. 2002 [cited 2022 Nov 6];2(4):251–62. Available from: https://www.nature.com/articles/nri778

18. Day CL, Kaufmann DE, Kiepiela P, Brown JA, Moodley ES, Reddy S, et al. PD-1 expression on HIV-specific T cells is associated with T-cell exhaustion and disease progression. Nature 2006 443:7109 [Internet]. 2006 Aug 20 [cited 2022 Sep 26];443(7109):350–4. Available from: https://www.nature.com/articles/nature05115

19. Gettinger S, Herbst RS. B7-H1/PD-1 blockade therapy in non-small cell lung cancer: Current status and future direction. Cancer Journal (United States) [Internet]. 2014 [cited 2022 Sep 26];20(4):281–9. Available from: https://journals.lww.com/journalppo/Fulltext/2014/07000/B7_H1_PD_1_Blockade_Therapy_in_Non_Small_Cell_Lung.8.aspx

20. Mamalis A, Garcha M, Jagdeo J. Targeting the PD-1 pathway: A promising future for the treatment of melanoma. Arch Dermatol Res [Internet]. 2014 Mar 11 [cited 2022 Sep 26];306(6):511–9. Available from: https://link-springer-com.proxy.library.uu.nl/article/10.1007/s00403-014-1457-7

21. Cohen EEW, Soulières D, le Tourneau C, Dinis J, Licitra L, Ahn MJ, et al. Pembrolizumab versus methotrexate, docetaxel, or cetuximab for recurrent or metastatic head-and-neck squamous cell carcinoma (KEYNOTE-040): a randomised, open-label, phase 3 study. The Lancet. 2019 Jan 12;393(10167):156–67.

22. Thommen DS, Schumacher TN. T Cell Dysfunction in Cancer. Vol. 33, Cancer Cell. Cell Press; 2018. p. 547–62.

23. Darnell EP, Mooradian MJ, Baruch EN, Yilmaz M, Reynolds KL. Immune-Related Adverse Events (irAEs): Diagnosis, Management, and Clinical Pearls. Current Oncology Reports 2020 22:4 [Internet]. 2020 Mar 21 [cited 2022 Nov 17];22(4):1–11. Available from: https://link.springer.com/article/10.1007/s11912-020-0897-9

24. Naidoo J, Wang X, Woo K, … TIJ of C, 2017 undefined. Pneumonitis in patients treated with anti–programmed death-1/programmed death ligand 1 therapy. ncbi.nlm.nih.gov [Internet]. [cited 2022 Oct 31]; Available from: https://www.ncbi.nlm.nih.gov/pmc/articles/PMC5559901/

25. Morganstein DL, Lai Z, Spain L, Diem S, Levine D, Mace C, et al. Thyroid abnormalities following the use of cytotoxic T-lymphocyte antigen-4 and programmed death receptor protein-1 inhibitors in the treatment of melanoma. Clin Endocrinol (Oxf). 2017 Apr 1;86(4):614–20.

26. Osorio J, Ni A, Chaft J, Pollina R, … MKA of, 2017 undefined. Antibody-mediated thyroid dysfunction during T-cell checkpoint blockade in patients with non-small-cell lung cancer. Elsevier [Internet]. [cited 2022 Oct 31]; Available from: https://www.sciencedirect.com/science/article/pii/S0923753419319593

27. Montero Pérez O, Sánchez Escudero L, Guzmán Ramos MI, Aviñó Tarazona V. Hypophysitis secondary to pembrolizumab: a case report and review of the literature. Anticancer Drugs [Internet]. 2022 Jan 1 [cited 2022 Oct 31];33(1):94–9. Available from: https://journals.lww.com/anti-cancerdrugs/Fulltext/2022/01000/Hypophysitis_secondary_to_pembrolizumab__a_case.11.aspx

28. Routy B, le Chatelier E, Derosa L, Duong CPM, Alou MT, Daillère R, et al. Gut microbiome influences efficacy of PD-1-based immunotherapy against epithelial tumors. Science (1979). 2018 Jan 5;359(6371):91–7.

29. Strickler JH, Hanks BA, Khasraw M. Tumor mutational burden as a predictor of immunotherapy response: Is more always better? Clinical Cancer Research [Internet]. 2021 Mar 1 [cited 2022 Oct 31];27(5):1236–41. Available from: https://aacrjournals.org/clincancerres/article/27/5/1236/83517/Tumor-Mutational-Burden-as-a-Predictor-of

30. Han J, Duan J, Bai H, Wang Y, Wan R, Wang X, et al. TCR repertoire diversity of peripheral PD-1þCD8þ T cells predicts clinical outcomes after immunotherapy in patients with non–small cell lung cancer. Cancer Immunol Res [Internet]. 2020 Jan 1 [cited 2022 Oct 31];8(1):146–54. Available from: https://aacrjournals.org/cancerimmunolres/article/8/1/146/470082/TCR-Repertoire-Diversity-of-Peripheral-PD-1-CD8-T

31. Martinez-Outschoorn U, … MPPN reviews C, 2017 undefined. Cancer metabolism: a therapeutic perspective. nature.com [Internet]. [cited 2022 Nov 17]; Available from: https://idp.nature.com/authorize/casa?redirect_uri=https://www.nature.com/articles/nrclinonc.2016.60&casa_token=hOQ8PUgMICsAAAAA:8CYIb8ZHpZ6bwZLdw4ICJFL7Tsyp8fsjldYy4_-aiAyHoOBs_Ut7QdD3ktZkFDUAdse_YrYULikuW_qs

32. Heiden MGV, Cantley LC, Thompson CB. Understanding the warburg effect: The metabolic requirements of cell proliferation. Science (1979). 2009 May 22;324(5930):1029–33.

33. Fischer K, Hoffmann P, Voelkl S, Meidenbauer N, Ammer J, Edinger M, et al. Inhibitory effect of tumor cell–derived lactic acid on human T cells. Blood [Internet]. 2007 May 1 [cited 2022 Nov 17];109(9):3812–9. Available from: https://ashpublications.org/blood/article/109/9/3812/23601/Inhibitory-effect-of-tumor-cell-derived-lactic

34. Ohl K, Tenbrock K. Reactive Oxygen Species as Regulators of MDSC-Mediated Immune Suppression. Front Immunol. 2018 Oct 30;9:2499.

35. Nagaraj S, Youn JI, Gabrilovich DI. Reciprocal Relationship between Myeloid-Derived Suppressor Cells and T Cells. The Journal of Immunology [Internet]. 2013 Jul 1 [cited 2022 Nov 17];191(1):17–23. Available from: https://journals.aai.org/jimmunol/article/191/1/17/104447/Reciprocal-Relationship-between-Myeloid-Derived

36. Zhou X, Fang D, Liu H, Ou X, Zhang C, Zhao Z, et al. PMN-MDSCs accumulation induced by CXCL1 promotes CD8+ T cells exhaustion in gastric cancer. Cancer Lett. 2022 Apr 28;532:215598.

37. Tanaka A, Sakaguchi S. Regulatory T cells in cancer immunotherapy. Cell Research 2017 27:1 [Internet]. 2016 Dec 20 [cited 2022 Nov 17];27(1):109–18. Available from: https://www.nature.com/articles/cr2016151

38. Tirosh I, Izar B, Prakadan SM, Wadsworth MH, Treacy D, Trombetta JJ, et al. Dissecting the multicellular ecosystem of metastatic melanoma by single-cell RNA-seq. Science (1979) [Internet]. 2016 Apr 8 [cited 2022 Oct 28];352(6282):189–96. Available from: https://www.science.org/doi/10.1126/science.aad0501

39. Thommen DS, Koelzer VH, Herzig P, Roller A, Trefny M, Dimeloe S, et al. A transcriptionally and functionally distinct PD-1+ CD8+ T cell pool with predictive potential in non-small-cell lung cancer treated with PD-1 blockade. Nature Medicine 2018 24:7 [Internet]. 2018 Jun 11 [cited 2022 Oct 28];24(7):994–1004. Available from: https://www.nature.com/articles/s41591-018-0057-z

40. Dong D, Zheng L, Lin J, Zhang B, Zhu Y, Li N, et al. Structural basis of assembly of the human T cell receptor–CD3 complex. Nature 2019 573:7775 [Internet]. 2019 Aug 28 [cited 2022 Oct 26];573(7775):546–52. Available from: https://www.nature.com/articles/s41586-019-1537-0

41. Grosso J, Kelleher C, … THTJ of, 2007 undefined. LAG-3 regulates CD8+ T cell accumulation and effector function in murine self- and tumor-tolerance systems. Am Soc Clin Investig [Internet]. [cited 2022 Oct 26]; Available from: https://www.jci.org/articles/view/31184

42. Andersen MH, Schrama D, Thor Straten P, Becker JC. Cytotoxic T Cells. Journal of Investigative Dermatology. 2006 Jan 1;126(1):32–41.

43. Zhu J, Paul WE. Heterogeneity and plasticity of T helper cells. Cell Research 2010 20:1 [Internet]. 2009 Dec 15 [cited 2022 Oct 26];20(1):4–12. Available from: https://www.nature.com/articles/cr2009138

44. Miggelbrink AM, Jackson JD, Lorrey SJ, Srinivasan ES, Waibl-Polania J, Wilkinson DS, et al. CD4 T-Cell exhaustion: Does it exist and what are its roles in cancer? Clinical Cancer Research [Internet]. 2021 Nov 15 [cited 2022 Oct 26];27(21):5742–52. Available from: https://aacrjournals.org/clincancerres/article/27/21/5742/671760/CD4-T-Cell-Exhaustion-Does-It-Exist-and-What-Are

45. Chen Z, Ji Z, Ngiow SF, Manne S, Cai Z, Huang AC, et al. TCF-1-Centered Transcriptional Network Drives an Effector versus Exhausted CD8 T Cell-Fate Decision. Immunity. 2019 Nov 19;51(5):840-855.e5.

46. Siddiqui I, Schaeuble K, Chennupati V, Fuertes Marraco SA, Calderon-Copete S, Pais Ferreira D, et al. Intratumoral Tcf1+PD-1+CD8+ T Cells with Stem-like Properties Promote Tumor Control in Response to Vaccination and Checkpoint Blockade Immunotherapy. Immunity. 2019 Jan 15;50(1):195-211.e10.

47. Li J, He Y, Hao J, Ni L, Dong C. High Levels of Eomes Promote Exhaustion of Anti-tumor CD8+ T Cells. Front Immunol. 2018 Dec 18;9:2981.

48. Knudson KM, Pritzl CJ, Saxena V, Altman A, Daniels MA, Teixeiro E. NFκB-Pim-1-Eomesodermin axis is critical for maintaining CD8 T-cell memory quality. Proc Natl Acad Sci U S A [Internet]. 2017 Feb 28 [cited 2022 Oct 26];114(9):E1659–67. Available from: https://www.pnas.org/doi/abs/10.1073/pnas.1608448114

49. Yigit B, Wang N, Hacken E ten, Chen SS, Bhan AK, Suarez-Fueyo A, et al. SLAMF6 as a regulator of exhausted CD8+ T cells in cancer. Cancer Immunol Res [Internet]. 2019 Sep 1 [cited 2022 Oct 26];7(9):1485–96. Available from: https://aacrjournals.org/cancerimmunolres/article/7/9/1485/469541/SLAMF6-as-a-Regulator-of-Exhausted-CD8-T-Cells-in

50. Hajaj E, Zisman E, Tzaban S, Merims S, Cohen J, Klein S, et al. Alternative splicing of the inhibitory immune checkpoint receptor SLAMF6 generates a dominant positive form, boosting T-cell effector functions. Cancer Immunol Res [Internet]. 2021 Jun 1 [cited 2022 Oct 26];9(6):637–50. Available from: https://aacrjournals.org/cancerimmunolres/article/9/6/637/666176/Alternative-Splicing-of-the-Inhibitory-Immune

51. Mita Y, Kimura MY, Hayashizaki K, Koyama-Nasu R, Ito T, Motohashi S, et al. Crucial role of CD69 in anti-tumor immunity through regulating the exhaustion of tumor-infiltrating T cells. Int Immunol [Internet]. 2018 Nov 14 [cited 2022 Oct 26];30(12):559–67. Available from: https://academic.oup.com/intimm/article/30/12/559/5067178

52. Koyama-Nasu R, Wang Y, Hasegawa I, Endo Y, Nakayama T, Kimura MY. The cellular and molecular basis of CD69 function in anti-tumor immunity. Int Immunol [Internet]. 2022 Oct 5 [cited 2022 Oct 26];34(11):555–61. Available from: https://academic.oup.com/intimm/article/34/11/555/6605936

53. Wherry EJ, Ha SJ, Kaech SM, Haining WN, Sarkar S, Kalia V, et al. Molecular Signature of CD8+ T Cell Exhaustion during Chronic Viral Infection. Immunity. 2007 Oct 26;27(4):670–84.

54. Blackburn S, Shin H, Haining W, … TZN, 2009 undefined. Coregulation of CD8+ T cell exhaustion by multiple inhibitory receptors during chronic viral infection. nature.com [Internet]. [cited 2022 Oct 26]; Available from: https://idp.nature.com/authorize/casa?redirect_uri=https://www.nature.com/articles/ni.1679&casa_token=qt0zAhctDIYAAAAA:PfyhhIxtLM8OI8iMIwT_vWSEbwgZcyJfvKj-3JVN6uRU6g4oTgN183QVAgz-cHfCGxUfVKY8C5WGQ_hV

55. Barber D, Wherry E, Masopust D, Zhu B, Nature JA, 2006 undefined. Restoring function in exhausted CD8 T cells during chronic viral infection. nature.com [Internet]. [cited 2022 Oct 26]; Available from: https://idp.nature.com/authorize/casa?redirect_uri=https://www.nature.com/articles/nature04444&casa_token=k17DxkuYBdYAAAAA:DFV-w0QrKziG-WOB_CedA-AxnZmHgYY12E_g4mNKithPyaSUPU4JDVKgpCvYzIVXXBFKaIIv42dL1LNM

56. Utzschneider D, Charmoy M, Chennupati V, Immunity LP, 2016 undefined. T cell factor 1-expressing memory-like CD8+ T cells sustain the immune response to chronic viral infections. Elsevier [Internet]. [cited 2022 Oct 26]; Available from: https://www.sciencedirect.com/science/article/pii/S1074761316302941

57. Ribas A, Puzanov I, Dummer R, Schadendorf D, Hamid O, Robert C, et al. Pembrolizumab versus investigator-choice chemotherapy for ipilimumab-refractory melanoma (KEYNOTE-002): a randomised, controlled, phase 2 trial. Lancet Oncol. 2015 Aug 1;16(8):908–18.

58. Hodi FS, O'Day SJ, McDermott DF, Weber RW, Sosman JA, Haanen JB, et al. Improved Survival with Ipilimumab in Patients with Metastatic Melanoma. New England Journal of Medicine. 2010 Aug 19;363(8):711–23.

59. Hodi F, Chiarion-Sileni V, Gonzalez R, … JGTL, 2018 undefined. Nivolumab plus ipilimumab or nivolumab alone versus ipilimumab alone in advanced melanoma (CheckMate 067): 4-year outcomes of a multicentre. Elsevier [Internet]. [cited 2022 Oct 26]; Available from: https://www.sciencedirect.com/science/article/pii/S1470204518307009?casa_token=3bDgAjpdZsQAAAAA:UUEx8jnN76OWUr0NuJm7Q4iWNN6YzR44TNznWDQjT4hU3JYxzSZ_qx-M8oiuIER1XRJp0sKzBA

60. Sobhani N, Tardiel-Cyril DR, Davtyan A, Generali D, Roudi R, Li Y. CTLA-4 in Regulatory T Cells for Cancer Immunotherapy. Cancers 2021, Vol 13, Page 1440 [Internet]. 2021 Mar 22 [cited 2022 Oct 26];13(6):1440. Available from: https://www.mdpi.com/2072-6694/13/6/1440/htm

61. de Sousa Linhares A, Leitner J, Grabmeier-Pfistershammer K, Steinberger P. Not All Immune Checkpoints Are Created Equal. Front Immunol. 2018 Aug 31;9:1909.

62. Maecker HT, Frey T, Nomura LE, Trotter J. Selecting fluorochrome conjugates for maximum sensitivity. Cytometry Part A. 2004 Dec;62(2):169–73.

63. Parga-Vidal L, Behr FM, Kragten NAM, Nota B, Wesselink TH, Kavazović I, et al. Hobit identifies tissue-resident memory t cell precursors that are regulated by eomes. Sci Immunol [Internet]. 2021 Aug 19 [cited 2022 Nov 7];6(62):3533. Available from: https://www-science-org.proxy.library.uu.nl/doi/10.1126/sciimmunol.abg3533

64. Li G, Yang Q, Zhu Y, Wang HR, Chen X, Zhang X, et al. T-Bet and Eomes Regulate the Balance between the Effector/Central Memory T Cells versus Memory Stem Like T Cells. PLoS One [Internet]. 2013 Jun 27 [cited 2022 Nov 17];8(6):e67401. Available from: https://journals.plos.org/plosone/article?id=10.1371/journal.pone.0067401

65. Dunsford LS, Thoirs RH, Rathbone E, Patakas A. A Human In Vitro T Cell Exhaustion Model for Assessing Immuno-Oncology Therapies. Methods in Pharmacology and Toxicology. 2020;89–101.

66. Call ME, Wucherpfennig KW. Molecular mechanisms for the assembly of the T cell receptor–CD3 complex. Mol Immunol. 2004 Apr 1;40(18):1295–305.

67. Gao GF, Jakobsen BK. Molecular interactions of coreceptor CD8 and MHC class I: The molecular basis for functional coordination with the T-cell receptor. Immunol Today [Internet]. 2000 Dec 1 [cited 2022 Nov 1];21(12):630–6. Available from: http://www.cell.com/article/S0167569900017503/fulltext

68. Blank C, Mackensen A. Contribution of the PD-L1/PD-1 pathway to T-cell exhaustion: an update on implications for chronic infections and tumor evasion. Cancer Immunology, Immunotherapy 2006 56:5 [Internet]. 2006 Dec 29 [cited 2022 Nov 1];56(5):739–45. Available from: https://link-springer-com.proxy.library.uu.nl/article/10.1007/s00262-006-0272-1

69. Doumpas N, Lampart F, Robinson MD, Lentini A, Nestor CE, Cantù C, et al. TCF/LEF dependent and independent transcriptional regulation of Wnt/β-catenin target genes. EMBO J [Internet]. 2019 Jan 15 [cited 2022 Nov 1];38(2):e98873. Available from: https://onlinelibrary.wiley.com/doi/full/10.15252/embj.201798873

70. Wherry EJ, Ha SJ, Kaech SM, Haining WN, Sarkar S, Kalia V, et al. Molecular Signature of CD8+ T Cell Exhaustion during Chronic Viral Infection. Immunity. 2007 Oct 26;27(4):670–84.

71. Zajac AJ, Blattman JN, Murali-Krishna K, Sourdive DJD, Suresh M, Altman JD, et al. Viral Immune Evasion Due to Persistence of Activated T Cells Without Effector Function. Journal of Experimental Medicine [Internet]. 1998 Dec 21 [cited 2022 Nov 1];188(12):2205–13. Available from: http://www.jem.org

72. Ahmadzadeh M, Johnson LA, Heemskerk B, Wunderlich JR, Dudley ME, White DE, et al. Tumor antigen–specific CD8 T cells infiltrating the tumor express high levels of PD-1 and are functionally impaired. Blood. 2009 Aug 20;114(8):1537–44.

73. Odorizzi PM, Pauken KE, Paley MA, Sharpe A, John Wherry E. Genetic absence of PD-1 promotes accumulation of terminally differentiated exhausted CD8+ T cells. Journal of Experimental Medicine [Internet]. 2015 Jun 29 [cited 2022 Nov 1];212(7):1125–37. Available from: www.jem.org/cgi/doi/10.1084/jem.20142237

74. Blackburn SD, Shin H, Freeman GJ, Wherry EJ. Selective expansion of a subset of exhausted CD8 T cells by alphaPD-L1 blockade. Proc Natl Acad Sci U S A [Internet]. 2008 Sep 30 [cited 2021 Dec 23];105(39):15016–21. Available from: https://pubmed.ncbi.nlm.nih.gov/18809920/

75. Maurice NJ, Berner J, Taber AK, Zehn D, Prlic M. Inflammatory signals are sufficient to elicit TOX expression in mouse and human CD8+ T cells. JCI Insight [Internet]. 2021 Jul 8 [cited 2022 Oct 8];6(13). Available from: https://doi.org/10.1172/jci.insight.150744DS1

76. Koh J, Kim S, Woo YD, Song SG, Yim J, Han B, et al. TCF1+PD-1+ tumour-infiltrating lymphocytes predict a favorable response and prolonged survival after immune checkpoint inhibitor therapy for non-small-cell lung cancer. Eur J Cancer [Internet]. 2022 Oct 1 [cited 2022 Oct 31];174:10–20. Available from: http://www.ejcancer.com/article/S0959804922004245/fulltext

77. Yost KE, Satpathy AT, Wells DK, Qi Y, Wang C, Kageyama R, et al. Clonal replacement of tumor-specific T cells following PD-1 blockade. Nature Medicine 2019 25:8 [Internet]. 2019 Jul 29 [cited 2022 Oct 8];25(8):1251–9. Available from: https://www.nature.com/articles/s41591-019-0522-3

78. Lynn RC, Weber EW, Sotillo E, Gennert D, Xu P, Good Z, et al. c-Jun overexpression in CAR T cells induces exhaustion resistance. Nature 2019 576:7786 [Internet]. 2019 Dec 4 [cited 2022 Nov 6];576(7786):293–300. Available from: https://www-nature-com.proxy.library.uu.nl/articles/s41586-019-1805-z

79. Zippelius A, Batard P, Rubio-Godoy V, Bioley G, Liénard D, Lejeune F, et al. Effector Function of Human Tumor-Specific CD8 T Cells in Melanoma Lesions: A State of Local Functional Tolerance. Cancer Res [Internet]. 2004 Apr 15 [cited 2022 Nov 2];64(8):2865–73. Available from: https://aacrjournals.org/cancerres/article/64/8/2865/517868/Effector-Function-of-Human-Tumor-Specific-CD8-T

80. Krummel MF, Allison JP. CD28 and CTLA-4 have opposing effects on the response of T ceils to stimulation. Journal of Experimental Medicine. 1995 Aug 1;182(2):459–65.

81. Walunas TL, Lenschow DJ, Bakker CY, Linsley PS, Freeman GJ, Green JM, et al. Pillars article: CTLA-4 can function as a negative regulator of T cell activation. Immunity. 1994. 1: 405-413. J Immunol [Internet]. 2011 Oct 1 [cited 2022 Nov 2];187(7):3466–74. Available from: http://www.ncbi.nlm.nih.gov/pubmed/21934098

82. He X, Xu C. Immune checkpoint signaling and cancer immunotherapy. Cell Research 2020 30:8 [Internet]. 2020 May 28 [cited 2022 Aug 18];30(8):660–9. Available from: https://www.nature.com/articles/s41422-020-0343-4

83. Hajaj E, Eisenberg G, Klein S, Frankenburg S, Merims S, David I ben, et al. SLAMF6 deficiency augments tumor killing and skews toward an effector phenotype revealing it as a novel T cell checkpoint. Elife. 2020 Mar 1;9.

84. Baitsch L, Legat A, Barba L, Marraco SA, Rivals JP, Baumgaertner P, et al. Extended Co-Expression of Inhibitory Receptors by Human CD8 T-Cells Depending on Differentiation, Antigen-Specificity and Anatomical Localization. PLoS One [Internet]. 2012 Feb 8 [cited 2022 Nov 2];7(2):e30852. Available from: https://journals.plos.org/plosone/article?id=10.1371/journal.pone.0030852

85. Harly C, Kenney D, Ren G, Lai B, Raabe T, Yang Q, et al. The transcription factor TCF-1 enforces commitment to the innate lymphoid cell lineage. Nature Immunology 2019 20:9 [Internet]. 2019 Jul 29 [cited 2022 Nov 3];20(9):1150–60. Available from: https://www.nature.com/articles/s41590-019-0445-7

86. Yu Q, Sharma A, Sen JM. TCF1 and β-catenin regulate T cell development and function. Immunologic Research 2010 47:1 [Internet]. 2010 Jan 16 [cited 2022 Nov 3];47(1):45–55. Available from: https://link.springer.com/article/10.1007/s12026-009-8137-2

87. Wang Y, Hu J, Li Y, Xiao M, Wang H, Tian Q, et al. The transcription factor Tcf1 preserves the effector function of exhausted CD8 T cells during chronic viral infection. Front Immunol. 2019;10(FEB):169.

88. Shan Q, Hu S, Chen X, Danahy DB, Badovinac VP, Zang C, et al. Ectopic Tcf1 expression instills a stem-like program in exhausted CD8+ T cells to enhance viral and tumor immunity. Cellular & Molecular Immunology 2020 18:5 [Internet]. 2020 Apr 27 [cited 2022 Nov 3];18(5):1262–77. Available from: https://www.nature.com/articles/s41423-020-0436-5

89. Giles JR, Ngiow SF, Manne S, Baxter AE, Khan O, Wang P, et al. Shared and distinct biological circuits in effector, memory and exhausted CD8+ T cells revealed by temporal single-cell transcriptomics and epigenetics. Nature Immunology 2022 23:11 [Internet]. 2022 Oct 21 [cited 2022 Nov 20];23(11):1600–13. Available from: https://www.nature.com/articles/s41590-022-01338-4

90. Koh J, Kim S, Woo YD, Song SG, Yim J, Han B, et al. TCF1+PD-1+ tumour-infiltrating lymphocytes predict a favorable response and prolonged survival after immune checkpoint inhibitor therapy for non-small-cell lung cancer. Eur J Cancer [Internet]. 2022 Oct 1 [cited 2022 Nov 6];174:10–20. Available from: http://www.ejcancer.com/article/S0959804922004245/fulltext

91. Sancho D, Gómez M, Sánchez-Madrid F. CD69 is an immunoregulatory molecule induced following activation. Trends Immunol. 2005 Mar 1;26(3):136–40.

92. Jutz S, Leitner J, Schmetterer K, Doel-Perez I, Majdic O, Grabmeier-Pfistershammer K, et al. Assessment of costimulation and coinhibition in a triple parameter T cell reporter line: Simultaneous measurement of NF-κB, NFAT and AP-1. J Immunol Methods. 2016 Mar 1;430:10–20.

93. Walsh DA, Borges da Silva H, Beura LK, Peng C, Hamilton SE, Masopust D, et al. The Functional Requirement for CD69 in Establishment of Resident Memory CD8 + T Cells Varies with Tissue Location . The Journal of Immunology [Internet]. 2019 Aug 15 [cited 2022 Oct 8];203(4):946–55. Available from: https://www.worldcat.org/title/8159288078

94. Pearce EL, Mullen AC, Martins GA, Krawczyk CM, Hutchins AS, Zediak VP, et al. Control of Effector CD8+ T Cell Function by the Transcription Factor Eomesodermin. Science (1979) [Internet]. 2003 Nov 7 [cited 2022 Oct 8];302(5647):1041–3. Available from: https://www.science.org/doi/10.1126/science.1090148

95. He H, Yi Y, Cai X, Wang J, Ni X, Fu Y, et al. Down-regulation of EOMES drives T-cell exhaustion via abolishing EOMES-mediated repression of inhibitory receptors of T cells in liver cancer. J Cell Mol Med [Internet]. 2021 Jan 1 [cited 2022 Oct 25];25(1):161–9. Available from: https://onlinelibrary.wiley.com/doi/full/10.1111/jcmm.15898

96. McLane LM, Ngiow SF, Chen Z, Attanasio J, Manne S, Ruthel G, et al. Role of nuclear localization in the regulation and function of T-bet and Eomes in exhausted CD8 T cells. Cell Rep. 2021 May 11;35(6):109120.

97. Gide TN, Quek C, Menzies AM, Tasker AT, Shang P, Holst J, et al. Distinct Immune Cell Populations Define Response to Anti-PD-1 Monotherapy and Anti-PD-1/Anti-CTLA-4 Combined Therapy. Cancer Cell [Internet]. 2019 Feb 11 [cited 2021 Dec 23];35(2):238-255.e6. Available from: https://pubmed.ncbi.nlm.nih.gov/30753825/

98. Hu G, Wang S. Tumor-infiltrating CD45RO+ Memory T Lymphocytes Predict Favorable Clinical Outcome in Solid Tumors. Scientific Reports 2017 7:1 [Internet]. 2017 Sep 4 [cited 2022 Oct 8];7(1):1–10. Available from: https://www.nature.com/articles/s41598-017-11122-2

99. Huard B, Prigent P, Tournier M, Bruniquel D, Triebel F. CD4/major histocompatibility complex class II interaction analyzed with CD4- and lymphocyte activation gene-3 (LAG-3)-Ig fusion proteins. Eur J Immunol. 1995;25(9):2718–21.

100. Krummel MF, Allison JP. CD28 and CTLA-4 have opposing effects on the response of T cells to stimulation. Journal of Experimental Medicine [Internet]. 1995 Aug 1 [cited 2022 Nov 21];182(2):459–65. Available from: http://rupress.org/jem/article-pdf/182/2/459/1107143/459.pdf

101. Saleh R, Elkord E. Treg-mediated acquired resistance to immune checkpoint inhibitors. Cancer Lett. 2019 Aug 10;457:168–79.

102. Janelle V, Neault M, Lebel MÈ, de Sousa DM, Boulet S, Durrieu L, et al. p16INK4a Regulates Cellular Senescence in PD-1-Expressing Human T Cells. Front Immunol. 2021 Aug 9;12:3131.

103. Wherry EJ, Kurachi M. Molecular and cellular insights into T cell exhaustion. Nature Reviews Immunology 2015 15:8 [Internet]. 2015 Jul 24 [cited 2022 Oct 24];15(8):486–99. Available from: https://www.nature.com/articles/nri3862

104. Vodnala SK, Eil R, Kishton RJ, Sukumar M, Yamamoto TN, Ha NH, et al. T cell stemness and dysfunction in tumors are triggered by a common mechanism. Science (1979) [Internet]. 2019 Mar 29 [cited 2022 Nov 7];363(6434). Available from: https://www.science.org/doi/10.1126/science.aau0135

105. Phan AT, Doedens AL, Palazon A, Tyrakis PA, Cheung KP, Johnson RS, et al. Constitutive Glycolytic Metabolism Supports CD8+ T Cell Effector Memory Differentiation during Viral Infection. Immunity. 2016 Nov 15;45(5):1024–37.

106. Nabe S, Yamada T, Suzuki J, Toriyama K, Yasuoka T, Kuwahara M, et al. Reinforce the antitumor activity of CD8+ T cells via glutamine restriction. Wiley Online Library [Internet]. 2018 Dec 1 [cited 2022 Nov 7];109(12):3737–50. Available from: https://onlinelibrary.wiley.com/doi/abs/10.1111/cas.13827

Supplementary Table 1 - Blood donor characteristics

Age	Sex
19	M
22	F
22	M
22	M
27	Unknown
30	M
30	F
30	M
34	F
36	M
36	F
39	M
39	F
40	F
42	F
43	M
53	M
60	F
61	F

Median Age	36
% sex Male	47
% sex Female	47
% sex Unknown	6

Supplementary Table 2 - Key Resources

REAGENT or RESOURCE	SOURCE	IDENTIFIER
Cell Culture Reagents		
RPMI-1640 medium	Capricorn Scientific	*Cat#RPMI-XA*
Fetal Bovine Serum	Bodinco BV	*Cat#S007V20007*
Penicillin-Streptomycin	Sigma-Aldrich	*Cat#P0781-100ML*
L-glutamine	Sigma-Aldrich	*Cat#G7513-100ML*
Trypsin-EDTA	Sigma-Aldrich	*Cat#T3924-100ML*
Dulbecco's Phosphate-buffered saline	Sigma-Aldrich	*Cat#D8537-500ML*
Dimethyl sulfoxide	Merck	*Cat#23488.294*
Türk Liquid	Merck Millipore	*Cat#1.09277.0100*
Trypan Blue 0.4%	Invitrogen	*Cat#* T10282
REAGENT or RESOURCE	SOURCE	
Chemicals, Peptides and Recombinant Proteins		
Fixable LIVE/DEAD nIR 780	Thermo Fisher	*Cat#L34992*
Pan-T cell isolation kit	Miltenyi Biotec	*Cat#130-096-535*
Recombinant human IL-2	Immunotools	*Cat#11340025*
Ficoll®Paque Plus	Sigma-Aldrich	*Cat#17-1440-03*
Phorbol-13myristate-14-acetate (PMA)	Merck Life Sciences	*Cat#79346-1MG*
Ionomycin	Merck Life Sciences	*Cat#I3909-1ML*
Phytohemaglutinin-L	Oxoid BV	*Cat#R30852801*
REAGENT or RESOURCE	SOURCE	IDENTIFIER
Critical Commercial Assays		
Foxp3/Transcription Factor Staining Buffer set	Invitrogen™	*Cat#00-5523-00*
MS column	Miltenyi Biotec	*Cat#130-042-201*
MiniMACS™ separator	Miltenyi Biotec	*Cat#130-042-102*
MACS® MultiStand	Miltenyi Biotec	*Cat#130-042-303*
Pan-T cell Isolation kit (human)	Miltenyi Biotec	*Cat#130-096-535*
REAGENT or RESOURCE	SOURCE	IDENTIFIER
Experimental Models: Cell Lines		
HEK293T	Grown in house	N/A
REAGENT or RESOURCE	SOURCE	IDENTIFIER
Deposited Data		
FACS FCS files	In this paper	https://umcu.elabjournal.com/members/experiments/?projectID=clear&studyID=97720

REAGENT or RESOURCE	SOURCE	IDENTIFIER
Software and Algorithms		
Biorender	Biorender Sotfware	https://biorender.com
GraphPad Prism v8	GraphPad Software	https://www.graphpad.com/scientific-software/prism/
Cytobank	Cytobank, Inc.	https://premium.cytobank.org/
REAGENT or RESOURCE		IDENTIFIER
Antibodies (Human, Intracellular, In Vivo)		
BV605 mouse anti-human CD4 (clone SK3)	Biolegend	Cat#344646
PerCP CD3 mouse anti-human (clone HIT3A)	Biolegend	Cat#300326
BV711 CD8 mouse anti-human (clone SK1)	Biolegend	Cat#344734
FITC PD-1 mouse anti-human (clone NAT105)	Biolegend	Cat#367412
BD Horizon™ Red 718 mouse anti-human/mouse TCF1/7	BD Biosciences	Cat#567587
PE TOX human anti-human/mouse (clone REA473)	Miltenyi Biotec	Cat#130-120-716
APC Slamf6 mouse anti-human (clone #292811)	R&D Systems	Cat#FAB19081A
BV650 LAG-3 (CD223) mouse anti-human (clone 11C3C8)	Biolegend	Cat#369606
BV510 CD69 mouse anti-human (clone FN50)	Biolegend	Cat#310936
PE-Cy7 EOMES mouse anti-human (clone WD1928)	ThermoFisher	Cat#25-48842
REAGENT or RESOURCE	SOURCE	IDENTIFIER
Biological Samples		
Whole blood donor samples	In-house donation	*N/A*
REAGENT or RESOURCE	SOURCE	IDENTIFIER
Software and Algorithms		
Biorender	Biorender Sotfware	https://biorender.com
GraphPad Prism v8	GraphPad Software	https://www.graphpad.com/scientific-software/prism/
Cytobank	Cytobank, Inc.	https://premium.cytobank.org/

Supplementary Figure 3 - T cell exhaustion flow panel compensation

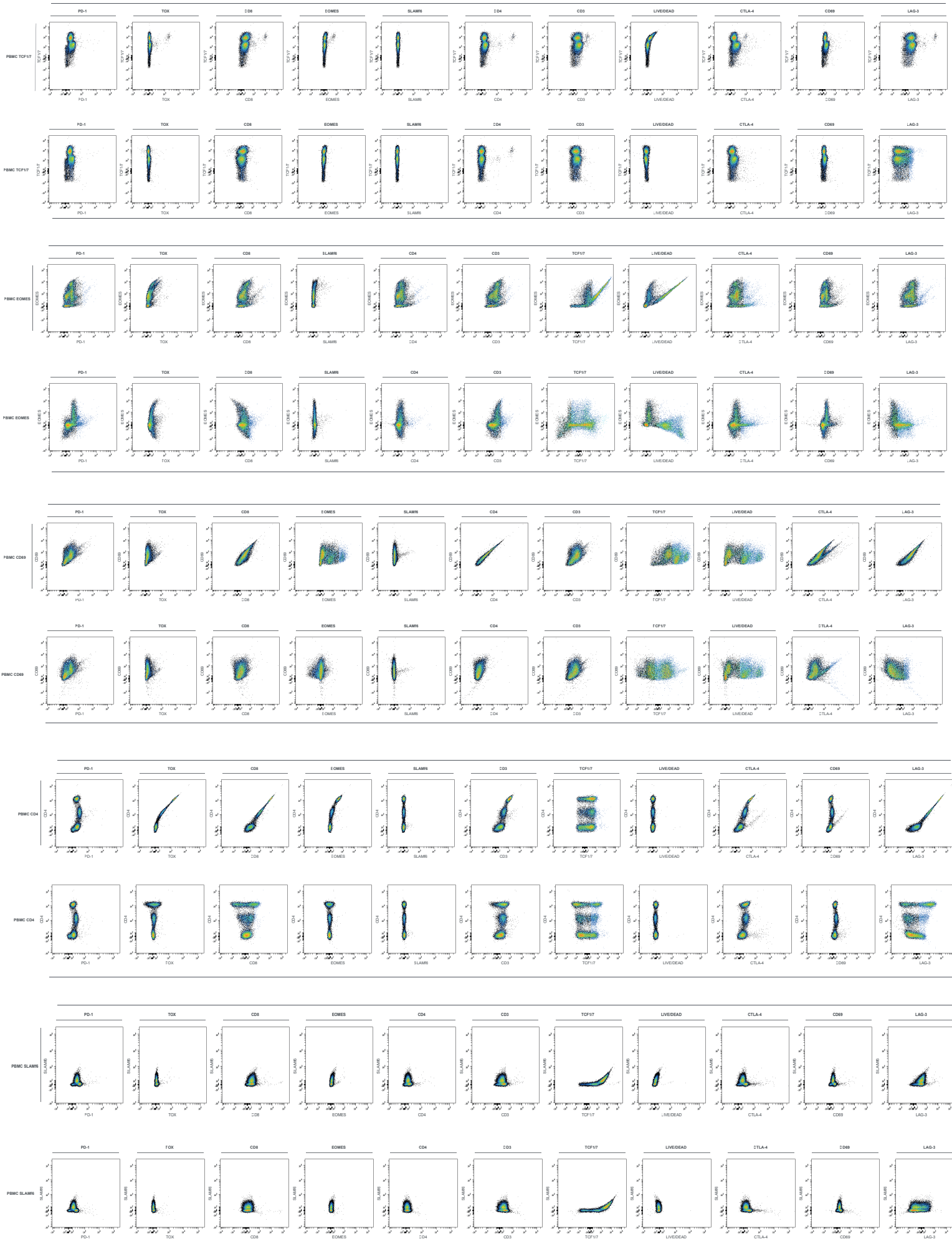

Supplementary Figure 1 T cell exhaustion flow panel compensation

T cell exhaustion panel markers before and after performing compensation. All plots show single staining of the respective marker. Staining was done using the Foxp3 Transcription Bu□er Set (eBioscience). PBMCs were stimulated for 3 days in PHA (5 mg/mL). A) TCF1/7 before (upper plots) and after (lower plots) against all other markers. B) Eomes before (upper plots) and after (lower plots) against all other markers. C) CD69 before (upper plots) and after (lower plots) against all other markers. D) CD4 before (upper plots) and after (lower plots) against all other markers. E) Slamf6 before (upper plots) and after (lower plots) against all other markers. and after (lower plots) against all other markers. (Figure continues on next page)

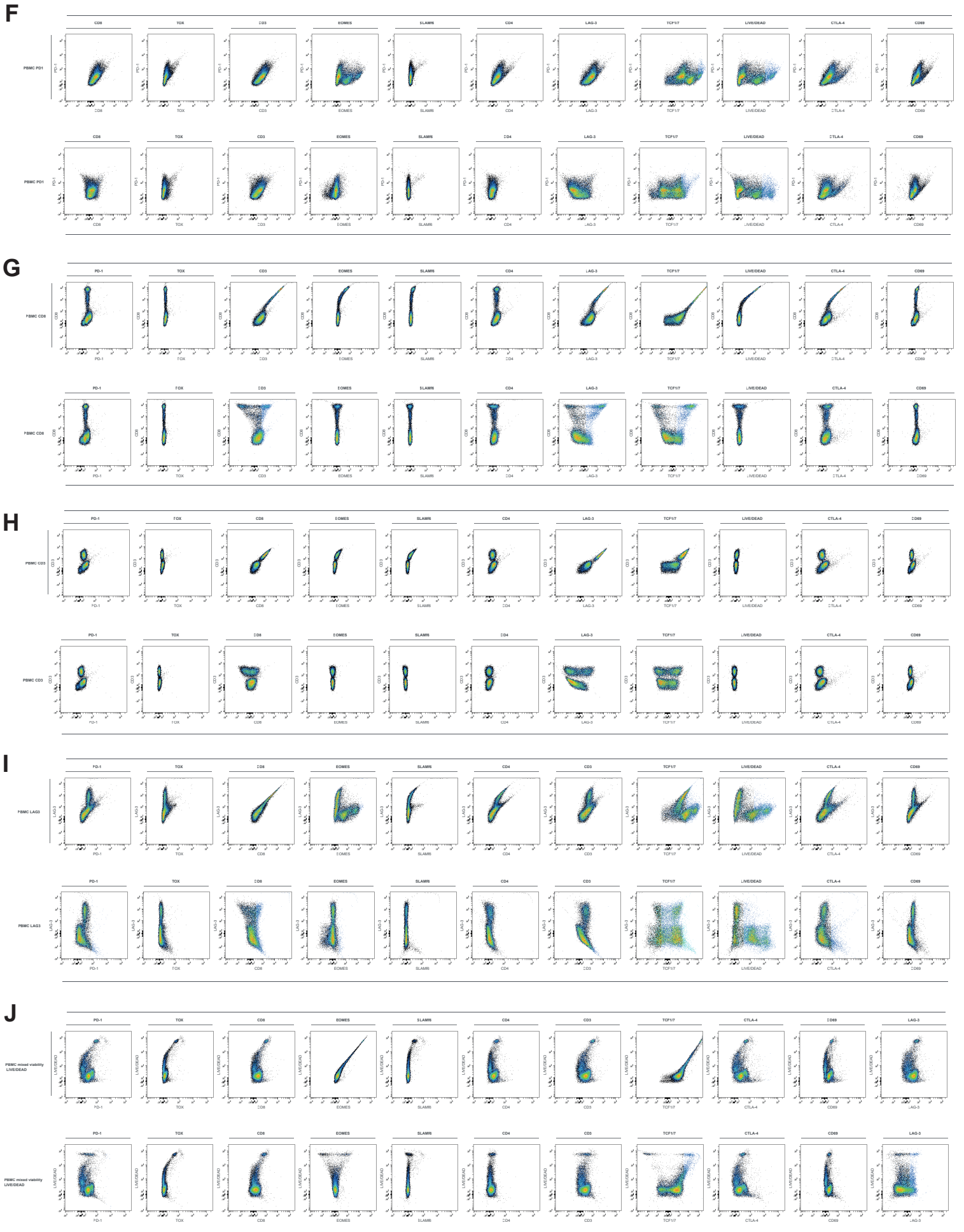

Supplementaryt 1: T cell exhaustion panel staining compensations (continued)

F) PD-1 before (upper plots) and after (lower plots) against all other markers. G) CD8 before (upper plots) and after (lower plots) against all other markers. H) CD3 before (upper plots) and after (lower plots) against all other markers. I) LAG-3 before (upper plots) and after (lower plots) against all other markers. J) LIVE/DEAD before (upper plots)

Figure continues on next page ->

K

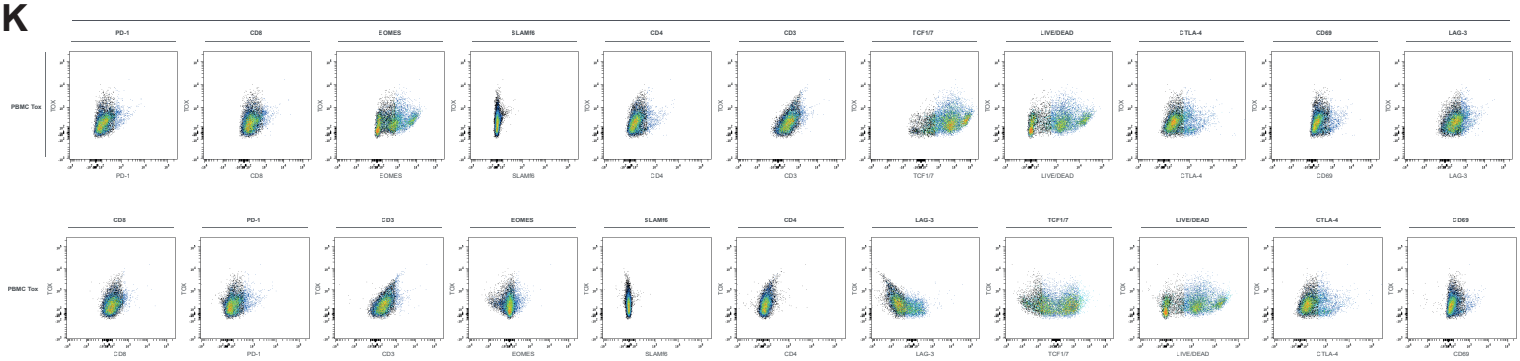

L

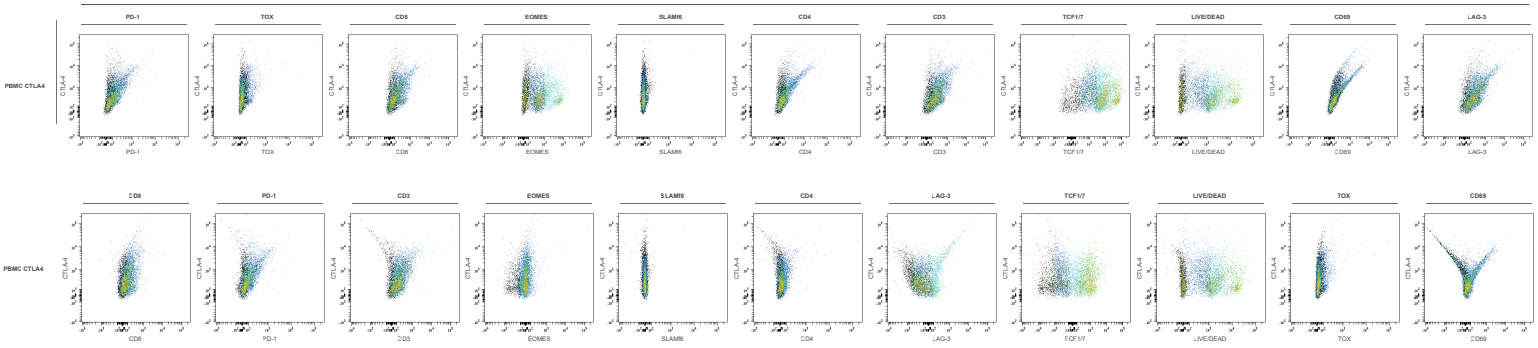

M

	FITC-A	PE-A	BV-711-A	PE-Cy7-A	APC-A	BV-605-A	PerCP-A	Alexa Fluor 700-A	APC-H7-A	Pacific Blue-A	BV-510-A	BV-650-A
FITC-A	100.0	2.0	10.0	2.0	0.0	8.0	20.0	23.0	8.0	14.00	10.0	0.0
PE-A	0.0	100.0	0.0	0.0	0.0	0.3	0.0	0.0	0.0	0.0	0.0	0.0
BV-711-A	0.0	0.0	100.0	0.6	0.1	0.0	17.0	205.00	1.9	2.80	0.1	6.7
PE-Cy7-A	0.0	3.1	3.8	100.0	0.0	0.0	2.0	10.0	1.80	0.0	0.0	-3.0
APC-A	0.0	0.0	0.0	10.65	100.0	0.0	0.0	0.0	0.0	5.64	0.0	57.51
BV-605-A	0.0	14.7	67.5	3.50	0.0	100.0	7.5	0.05	0.0	5.5	0.0	210.0
PerCP-A	0.0	0.0	51.0	5.0	4.8	0.0	100.0	123.0	1.0	0.0	0.0	200.0
Alexa Fluo	0.0	0.0	0.1	0.0	0.0	0.0	0.0	100.0	1.0	0.0	0.0	0.4
APC-H7-A	1.10	0.2	0.3	35.0	0.3	0.1	1.2	315.0	100.0	0.3	0.2	0.0
Pacific Blu	0.5	0.0	0.0	0.0	0.0	7.00	2.4	0.0	0.0	100.0	15.0	4.0
BV-510-A	0.0	0.0	30.0	0.0	0.0	50.00	0.0	0.0	0.0	43.0	100.0	85.0
BV-650-A	0.1	0.1	35.62	0.5	0.70	3.0	1.3	29.4	0.3	2.0	0.0	100.0

Fig. 2 T cell exhaustion panel antibody testing and titration. (continued)
K) Tox before (upper plots) and after (lower plots) against all other markers. L) CTLA-4 before (upper plots) and after (lower plots) against all other markers M) Compensation Matrix values.

Supplementary Table 4 - Flow Cytometry Panel configuration

Laser	Antibody	Fluorochrome	Firma	Clone
450/40 (405)	CTLA-4	BV421	Biolegend	BNI3
525/50 (405)	CD69	BV510	Biolegend	FN50
610/20 (405)	CD4	BV605	Biolegend	SK3
670/30 (405)	LAG-3	BV650	Biolegend	11C3C8
710/50 (405)	CD8	BV711	Biolegend	SK1
530/30 (488)	PD-1	FITC	Biolegend	NAT105
575/26 (488)	CD3	PerCP	Biolegend	HIT3A
586/15 (561)	TOX	PE	Miltenyi Biotec	REA473
610/20 (561)				
670/30 (561)				
710/50 (561)				
780/60 (561)	EOMES	PE-Cy7	ThermoFisher	WD1928
660/20 (633)	SLAMf6	APC	R&D Systems	292811
730/45 (633)	TCF1/7	Horizon Red 718	BD Biosciences	S33-966
780/60 (633)	LIVE/DEAD	nIR 780	ThermoFisher	-

Supplementary Table 4 - Panel configuration
Flow cytometry panels used for the charcterization of an in vitro T cell exhaustion model. A flow cytometry panel composed of directly fluorochrome-conjugated antibodies against different immunophenotypic markers was designed for the characterization of T cells. The antibodies were purchased from BD Biosciences (San Diego, CA, USA), R&D Systems (Minneapolis, MN, USA), Miltenyi Biotec (Leiden, The Netherlands), BioLegend (San Diego, CA, USA), Thermo Fisher Scientific (Waltham, Massachusetts, USA).

Abbreviations: APC (allophycocyanin), BV (brilliant violet), FITC (fluorescein isothiocyanate), nIR (near-infrared), PE (phycoerythrin), PE-Cy7 (phycoerythrin-cyanine7), PerCP (peridinin chlorophyll protein complex)

Supplementary Figure 5 - Expression of panel markers on negative control cell line

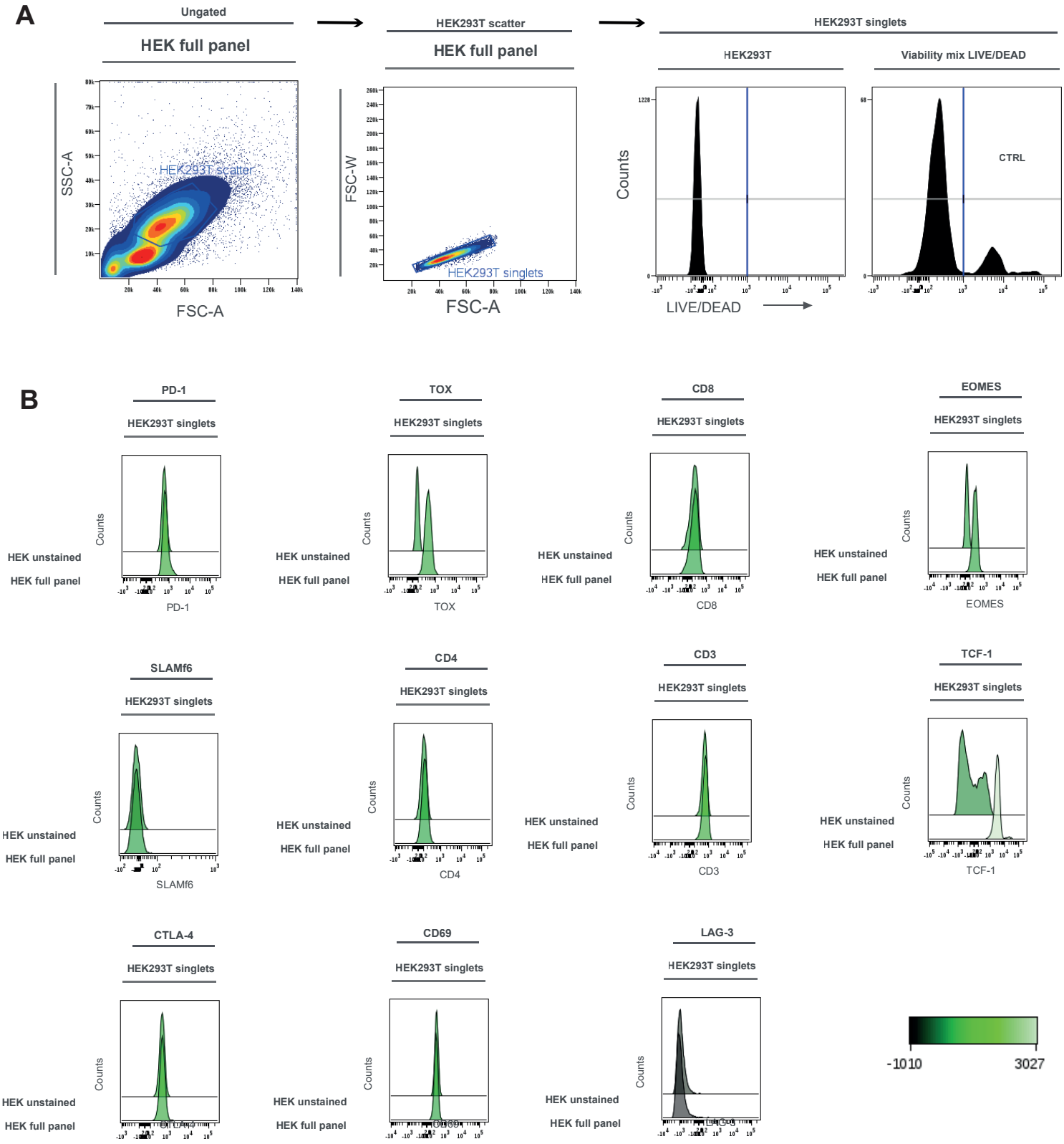

Supplementary Figure 5 - Expression of panel markers on negative control cell line
HEK293T cells were stained with the full flow cytometry panel and protocol used for the charcterization of an in vitro T cell exhaustion model. A) Gating strategy for HEK293T cells. B) Marker expression of all markers in T cell exhaustion panel. All markers show negative staining, except TCF-1.

Supplementary Figure 6 - Effects of culturing conditions on T cell viability

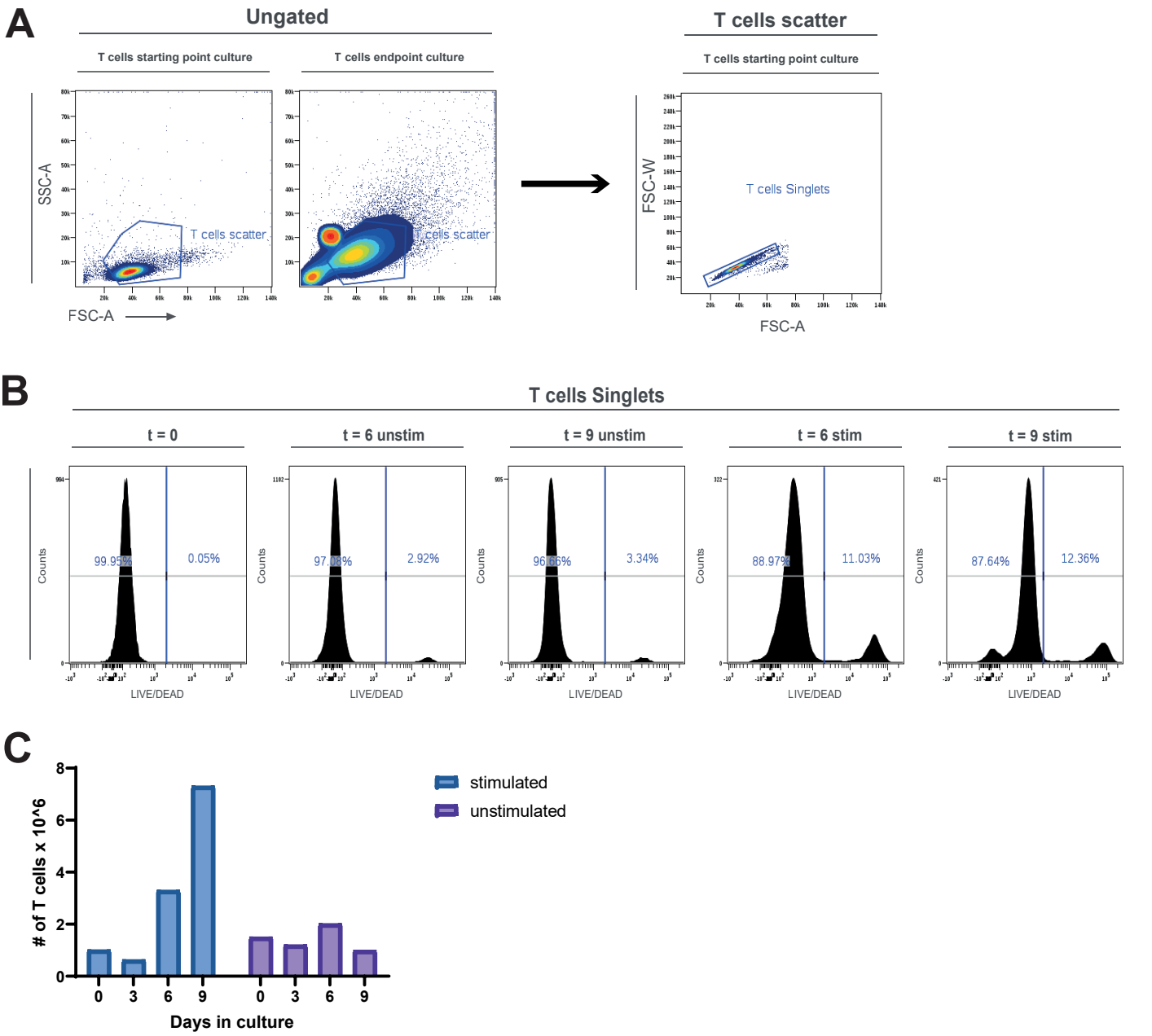

Supplementary Figure 2. Effects of culturing conditions on T cell viability
Viability is assessed by fraction of LIVE/DEAD+ or monitoring absolute cell numbers. A) Gating strategy for T cells, excluding debris and double events. B) Histograms representing live and dead cells at different timepoints and culturing conditions. C) Absolute numbers of live cells, by means of manual count in hematocytometer at different timepoints and culturing conditions.